Earth-Science Reviews 267 (2025) 105168

Contents lists available at ScienceDirect

Earth-Science Reviews

journal homepage: www.elsevier.com/locate/earscirev

Review Article

Degassing of deep fluids in the Pannonian basin and adjacent areas

Paolo Randazzo [a,*], Alessandro Aiuppa [b], Staša Borović [c], Dario Buttitta [a], Carlo Cardellini [d,e], Giovanni Chiodini [e], Artur Ionescu [d,f,g], Giancarlo Tamburello [e], Antonio Caracausi [a,*]

[a] Istituto Nazionale di Geofisica e Vulcanologia, Sezione di Palermo, Palermo, Italy
[b] Department of Earth and Marine Sciences, University of Palermo, Palermo, Italy
[c] Department of Hydrogeology and Engineering Geology, Croatian Geological Survey, Zagreb, Croatia
[d] Dipartimento di Fisica e Geologia, University of Perugia, Perugia, Italy
[e] Istituto Nazionale di Geofisica e Vulcanologia, Sezione di Bologna, Bologna, Italy
[f] Faculty of Biology and Geology, Department of Geology, Babeș-Bolyai University, Cluj-Napoca, Romania
[g] HUN-REN, Institute for Nuclear Research, Debrecen, Hungary

ARTICLE INFO

Keywords:
Pannonian basin
Carbon dioxide
Isotopic geochemistry
Noble gases
Water-gas interaction
Dissolution
Precipitation
Methanogenesis
Tectonic

ABSTRACT

The Pannonian Basin (PB), in Central-Eastern Europe, is a continental area characterized by widespread presence of natural resources, high heat fluxes and outgassing of deep-sourced fluids (i.e. mantle-magma and/or crustal-derived). Moreover, the region is interested by ascent of the asthenosphere and a thin lithosphere (≈75 km). Here, we review 40 years of geochemical studies on natural gas emissions in the PB system and nearby areas providing the first comprehensive geochemical characterization of gas manifestations for the Croatian segment of PB. We use stable isotope ($\delta^{13}C_{CO2}$) geochemistry, noble gases data, and C—He systematics to reconcile geochemical information with geophysical and geodynamic models at regional scale, and hence to characterize (i) the source/s of fluids outgassing at the surface and (ii) the main processes occurring during their storage in, and transit through, the crust.

The chemical composition of the emitted fluids is very heterogeneous in the PB. We identify three distinct gas types (CO_2-dominated, N_2-dominated, and CH_4-dominated) that are variably distributed in different sectors of PB. The He isotopic composition range from 0.07 to 6.32Ra (Ra is the air He isotopic signature), suggesting the coexistence of crustal and mantle components in the area. Furthermore, the same components also occur in the Croatian PB, where the He isotopic ratios range from 0.02 Ra to 2.21 Ra. The groundwater circulation in the PB implies an addition of atmospheric-derived noble gas component to the deep fluids (mantle vs crust-derived). The volumetric gas/water ratios (Vg/Vl) are highly variable (0.002 to 66) with the highest values in N_2-dominated samples, and correlate with atmospheric-derived ^{20}Ne concentration, pointing to shallow gas origin for these samples (relative to CO_2 and CH_4-dominated samples). The C—He systematics, coupled with the $\delta^{13}C$ of CO_2, indicates extensive chemical and isotopic fractionation due to partial dissolution of gas in water in the shallow crustal layers and consequent CO_2 trapping in deep aquifers and/or in precipitating carbonates. In addition, methanogenesis could work as an additional potential CO_2 sink in the crust. The mantle-derived He flux, on a regional scale, is estimated at 1.7×10^{10} to 1.7×10^{12} atoms m^{-2} s^{-1}, one order of magnitude greater than found by O'Nions and Oxburgh (1988), and similar to what found in other tectonically active regions. The mantle-related CO_2 flux computed using $CO_2/^3He$ ratios and the mantle He fluxes, range between 10^3 and 10^5 mol·km^{-2}·$year^{-1}$. Despite representing a rough estimation, these values are in the range of the CO_2 fluxes in active and quiescent worldwide volcanic systems. We propose the transfer of mantle-derived volatiles to occurs through lithospheric faults in the PB and adjacent regions, although the presence of magmatic intrusions in crustal layers is an additional contributing factor.

Contents

* Corresponding authors.
E-mail address: paolo.randazzo@ingv.it (P. Randazzo).

https://doi.org/10.1016/j.earscirev.2025.105168
Received 9 July 2024; Received in revised form 15 May 2025; Accepted 18 May 2025
Available online 22 May 2025

1. Introduction

Over the past few decades, the degassing of natural fluids in continental regions, both volcanically (e.g., Alonso et al., 2022; Kimani et al., 2021; Aiuppa et al., 2021; Werner et al., 2019; Chiodini et al., 2008, Chiodini et al., 2021a, 2021b) and seismically active (e.g., Chiodini et al., 2004, 2011, 2020; Rufino et al., 2021; Zhang et al., 2021; Caracausi et al., 2022; Buttitta et al., 2023), has received increasing attention. The accurate quantification of geogenic gas emissions into the atmosphere is a key to assessing the global budget of volatiles and the role of fluids in natural processes, such as volcanic eruptions and earthquakes. Furthermore, the chemical and isotopic composition of fluids (e.g., CO_2, N_2, noble gases) provides valuable insights into the different processes responsible for the Earth evolution—such as subduction, volcanism, metamorphism, and tectonics (e.g., Barry et al., 2021; Broadley et al., 2020; Labidi et al., 2020; Chiodini et al., 2020; Caracausi and Sulli, 2019; Newell et al., 2008; Ballentine et al., 2001)—and supports the exploration and exploitation of natural resources (Ballentine et al., 1991; Sherwood et al., 1994, 1997; Vető et al., 2004).

The Pannonian basin (PB), in Central-Eastern Europe (CEE), located at the convergence between the Eurasian and Nubian plates (Horváth et al., 2015), represents a tectonically active region with ongoing neotectonic processes, exhibiting geothermal anomalies and heat flows ranging from 50 to 130 mW m^{-2} (Koroknai et al., 2020). The region hosts significant geothermal resources and hydrocarbon fields (Horváth et al., 2015).

During the last forty years, several geochemical investigations have been carried out in the CEE focused on gas and hydrocarbon exploitation (e.g., Ballentine et al., 1991; Sherwood et al., 1994, 1997) and for exploring Earth degassing in active tectonic regions (e.g., Randazzo et al., 2021; Sarbu et al., 2018; Ionescu et al., 2017; Italiano et al., 2017; Frunzeti, 2013; Bräuer et al., 2008). Early studies (Cornides and Kecskés, 1982; Cornides, 1983) identified widespread deep-sourced CO_2 degassing in the PB, primarily from mantle sources, and highlighted some correlations between degassing, crustal thinning and high heat flows. These observations were further supported by O'Nions and Oxburgh (1988) who investigated the distribution of primordial helium (He) in the european continental regions, including the PB, to explore the release of mantle fluids in tectonically active areas far from volcanoes and confirmed the correlation between tectonic activity and mantle-derived He in the continental crust, an evidence that has been confirmed in more than 30 years of studies worldwide (e.g., Poreda et al., 1986; Mamyrin and Tolstikhin, 1984; Torgersen, 1993; Caracausi et al., 2005, 2022; Güleç and Hilton, 2006; Kulongosky et al., 2005, 2013; Mutlu et al., 2008; Tamburello et al., 2018). The mantle He fluxes in the PB, reaching up to 10^8 atoms m^{-2} s^{-1} (O'Nions and Oxburgh, 1988), are characteristic of extensional tectonic settings with degassing from asthenospheric melts or directly from the mantle (e.g., Burnard et al., 2013).

Additional studies during the 1990s (e.g., Ballentine et al., 1991; Sherwood et al., 1994, 1997) confirmed the presence of mantle-derived He and CO_2 components in the PB gas fields. Recent investigations (e.g., Vető et al., 2014; Palcsu et al., 2014; Bräuer et al., 2016) refined these findings, identifying mantle/magmatic CO_2 mixing with crustal fluids and the highest $^3He/^4He$ ratios (4.95–6.32 Ra) on the Austria-Slovenia border area within the PB. These values are indicative of magmatic reservoirs with a Sub-Continental Lithospheric Mantle (SCLM) signature (Bräuer et al., 2016). Similarly, the occurrence of mantle-derived He was also observed in Serbia (e.g. Vardar Zone, Randazzo et al., 2021), where the mantle-He fluxes exceed those in stable continental areas by two orders of magnitude. Although several geochemical studies investigated fluids in the Croatian sector of the PB (e.g., Fiket et al., 2015; Borović et al., 2016), the origin of natural fluids emitted in this region remain poorly understood, and a comprehensive regional model about the origin of the main volatiles in the PB and about the processes that modify the chemistry of the fluids at depth is missing.

The combination of crustal and mantle degassing, high heat fluxes, and surface hydrothermal manifestations makes the PB an ideal area for the geothermal resources exploitation, exploration of new natural resources such as He and H_2, and studies on climate change and atmospheric CO_2 budget. Furthermore, from a multidisciplinary point of view, the PB represents a natural laboratory for examining the tectonic evolution of intra-orogenic basins, as well as the lithospheric structure and tectonic dynamics in extensional and collisional settings (Kalmár et al., 2023). This study aims to fill the gap in knowledge by integrating the existing geochemical data with new ones from the Croatian sector of the PB. By integrating these data with geophysical and geodynamic models, we seek to offer a comprehensive regional reconstruction of fluid origin and the processes that modify their chemical and isotopic composition within the crust. This work will contribute to ongoing efforts in natural resources exploration and provide a better understanding of the complex geodynamic evolution of the Pannonian Basin.

2. Geological setting

The evolution of the PB is related to the interaction between the Eurasian and Nubian plates. The area was shaped by a complex sequence of geodynamic and tectonic events, such as active subduction, continental collision, extension and formation of back arc basins, which developed from the middle Mesozoic until the present day (Schmid

et al., 2020 and references therein). The geodynamic evolution of the PB can be divided into two main phases. The first phase, spanning from the middle Permian to the early Miocene, is related to the Alpine orogeny and the collision between the European Platform, the Adriatic microplate and the African Plate (Rman et al., 2020 and references therein). This collision resulted in complex suture zones of different ages (e.g. Sava zone, Vardar zone) formed by nappe systems with different vergences, coupled to numerous crustal blocks and several oceanic crust fragments that constitute the basement of the later PB (Horváth et al., 2015). The second phase comprises the formation of the back-arc type PB, which started in the early-middle Miocene and lasted until recent times. Evolutionary models assume the onset of extension at approximately 20 Ma, followed by a peak in the tectonic activity along normal faults during the middle Miocene. This was subsequently followed by a post rift, thermal sag phase starting in the late Miocene (Matenco and Radivojevic, 2012; Tari et al., 1999). Most of the extension was accommodated by the rapid rollback of the Carpathian slab from 20 Ma to 9 Ma ago (e.g., Csontos, 1995; Fodor et al., 1999; Merten et al., 2010; Horváth et al., 2018). At the beginning of the Pliocene, subduction practically ceased due to the gradual increase in the subduction dip angle and a northward compression of the Adria microplate, which simultaneously rotated counterclockwise (Balázs et al., 2016 and reference therein). As a result of all these processes, a compressive tectonic regime developed within the PB (Lenkey et al., 2002; Grenerczy et al., 2005; Bada et al., 2007; Koroknai et al., 2020). Magmatism in the Carpathian-Pannonian system also exhibited spatial and temporal heterogeneity. Models based on petrological and geochemical data recognize a general temporal transition from felsic calc-alkaline, mafic to intermediate calc-alkaline, to alkali-basalts, basanite and ultrapotassic magmatism (e.g., Konecny et al., 2002; Koptev et al., 2021).

The crust beneath the PB is relatively thin, generally ranging from 25 to 30 km, whit the thinnest portion (25 Km) in the northeast (e.g., Ren et al., 2013 and references therein), likely resulting from a rift-dominated extension phase in the Miocene (Szafian et al., 1997; Huismans et al., 2001). Lithospheric extension is also the origin of the regional high surface heat flow (50 mW m^{-2} to 130 mW m^{-2}; Hurter and Haenel, 2002; Horváth et al., 2015). Groundwater storage and circulation within the crust play a role in controlling the variability of the heat flows at the surface (Nádor et al., 2019). For years, several projects and studies have been aimed at investigating the deeper crustal layers, the crustal-mantle boundary and the geodynamic evolution of the PB area (e.g., CELEBRATION 2000 profiles, Godova et al., 2021; Tašarova et al., 2009; Bielik et al., 2005, 2006; Guterch et al., 2000a, 2000b). Recently, regional geophysical investigations have been recognized delamination processes and urderthrusting in different areas of South-eastern Europe, accompanied by lithospheric thinning and ascent of hotter asthenospheric material in the PB area (Belinić et al., 2021). In particular, the PB system is characterized by one of the thinnest continental crusts and

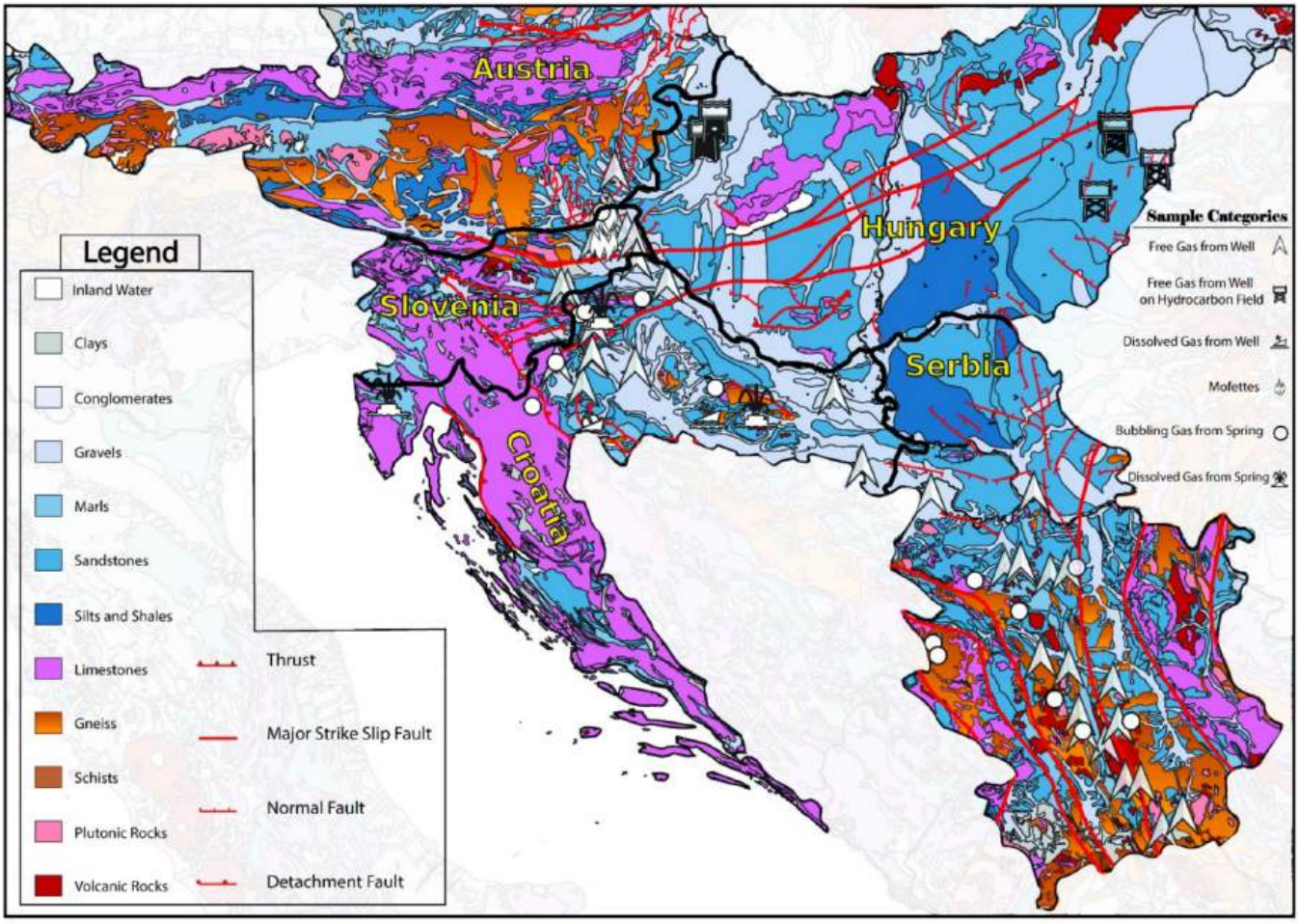

Fig. 1. Simplified geological map of the Pannonian basin and Vardar zone area with major regional tectonic discontinuities (BGR & UNESCO (eds.) (2014): International Hydrogeological Map of Europe 1:1,500,000 (IHME1500). Digital map data v1.1. Hannover/Paris; tectonic discontinuities from The European Database of Seismogenic Faults, EDSF). The sample locations and sample categories are also shown. Literature data from Randazzo et al., 2021, Bräuer et al., 2016, Sherwood et al., 1997, Vető et al., 2014 and Ballentine et al., 1991 for Serbia, Austria-Slovenia and Hungary respectively. Data discussed in the text as unpublished data are all those falling within the Croatia boundaries.

lithospheres (~75 km) in the world (Bielik et al., 2022), with melting occurring in the asthenosphere just below the thinned lithosphere (Bracco Gartner and McKenzie, 2020). It is worthy to note that the PB is still tectonically active as highlighted by GPS geodetic observations and seismic monitoring (Grenerczy et al., 2005; Tóth et al., 2006 and reference therein). Earthquake activity in the PB can be characterized as intraplate seismicity of moderate intensity with significant variations between different tectonic domains (Tóth et al., 2008). Earthquakes are predominantly clustered in the southeast Carpathians zone, where the highest magnitudes (three M > 6.5 within the last 30 years and yearly M = 5; Zsíros, 2003a, 2003b) are observed. The majority of the events occur between 6 km and 15 km depth, and the focal mechanisms are dominated by thrust and strike-slip faulting (Tóth et al., 2008).

3. Gas geochemistry

3.1. Chemical composition

The chemical and isotopic composition of 23 new gas samples collected in Croatia (Figs. 1 and 2), together with literature data (122 samples), are reported in Table S1 and Fig. 3. The sampling and analysis methods are described in the Supplementary material S1.

Based on their chemical composition it is possible to broadly classify these gases in three groups. The CO_2-dominated samples ($CO_2 > 50$ %) represent 53 % of the total 145 samples and are mainly located in Serbia, W-Hungary, and along the Austria-Slovenia border. The N_2-dominated samples ($N_2 > 50$ %) constitute 18 % of the total and are mainly localized in the Croatian sector of the PB (65 %) and the Serbian Vardar zone (Figs. 2 and 3). CH_4-dominated ($CH_4 > 50$ %) samples are 28 % of the total and most of them are located in correspondence to the *E*-Hungary hydrocarbon fields. Furthermore, on the western Serbia ophiolitic massifs, H_2-dominated bubbling gases from two hyperalkaline waters were encountered. These samples exhibit H_2 concentrations of 81–85 % (Randazzo et al., 2021). Fig. 4 shows that CO_2 amounts are negatively correlated with CH_4 and N_2, and that such CO_2 depletion exhibits two distinct trends.

3.2. Isotopic composition

3.2.1. Carbon

The CO_2 carbon isotopic composition of the PB samples is variable (-20.2 ‰ $< \delta^{13}C_{CO2} < +12.8$ ‰; Table S1 and Fig. S1 Supplementary materials) and overlaps the mantle (-10 ‰ $\leq \delta^{13}C_{CO2} \leq -1$ ‰) and metamorphic (-4 ‰ $\leq \delta^{13}C_{CO2} \leq +3$ ‰) ranges (Clark and Fritz, 2013). The N_2-dominated and H_2-dominated gases from Croatia and Serbia exhibit the most negative $\delta^{13}C_{CO2}$ values (down to -20.2 ‰ for N_2-dominated and -17.1 ‰ for H_2-dominated gases), which is within the range of biogenic CO_2. Two Croatian samples (CRT7 and CRT8, CO_2 and CH_4 dominated respectively) have unusually positive CO_2 carbon isotopic composition ($\delta^{13}C_{CO2}$ of +10.6 ‰ and + 12.8 ‰, respectively), which could reflect oil-biodegradation processes (Milkov, 2020).

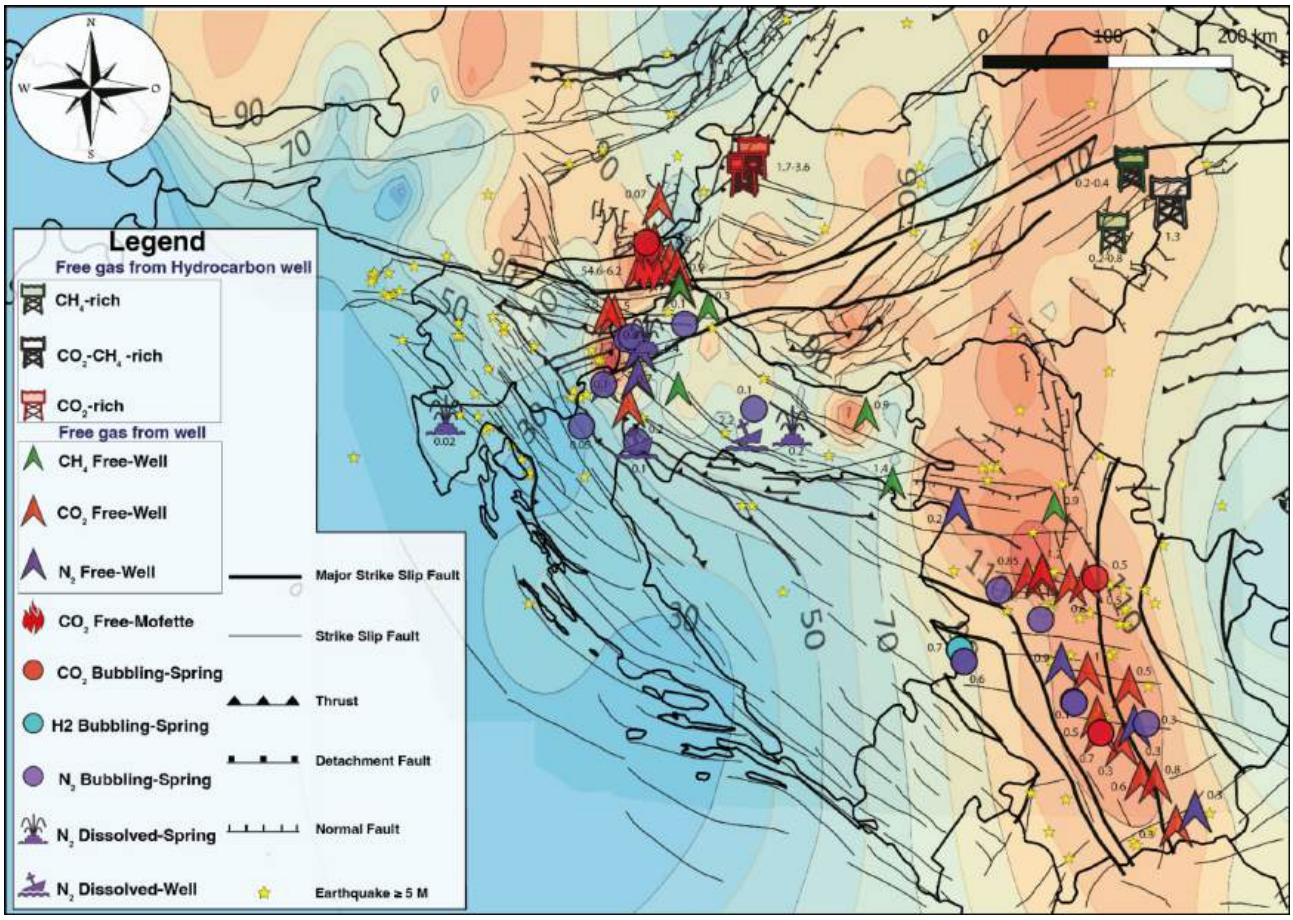

Fig. 2. Heat flow map of the Pannonian basin and surrounding regions (heat flow values in mW/m^2; Horváth et al., 2015, Lenkey et al., 2002). Major and minor tectonic discontinuities are also shown. The sample categories are the same as Fig. 1. Different colors denote different chemical composition: Red = CO_2-dominated, Green = CH_4-dominated; Purple = N_2-dominated; Ciano = H_2-dominated. Black numbers are the Rc/Ra values. Yellow stars show earthquakes≥5 M (Markušić, 2008, Tóth et al., 2008; http://www.seismo.gov.rs/Seizmicnost/Katalog-zemljotresa.pdf). (For interpretation of the references to colour in this figure legend, the reader is referred to the web version of this article.)

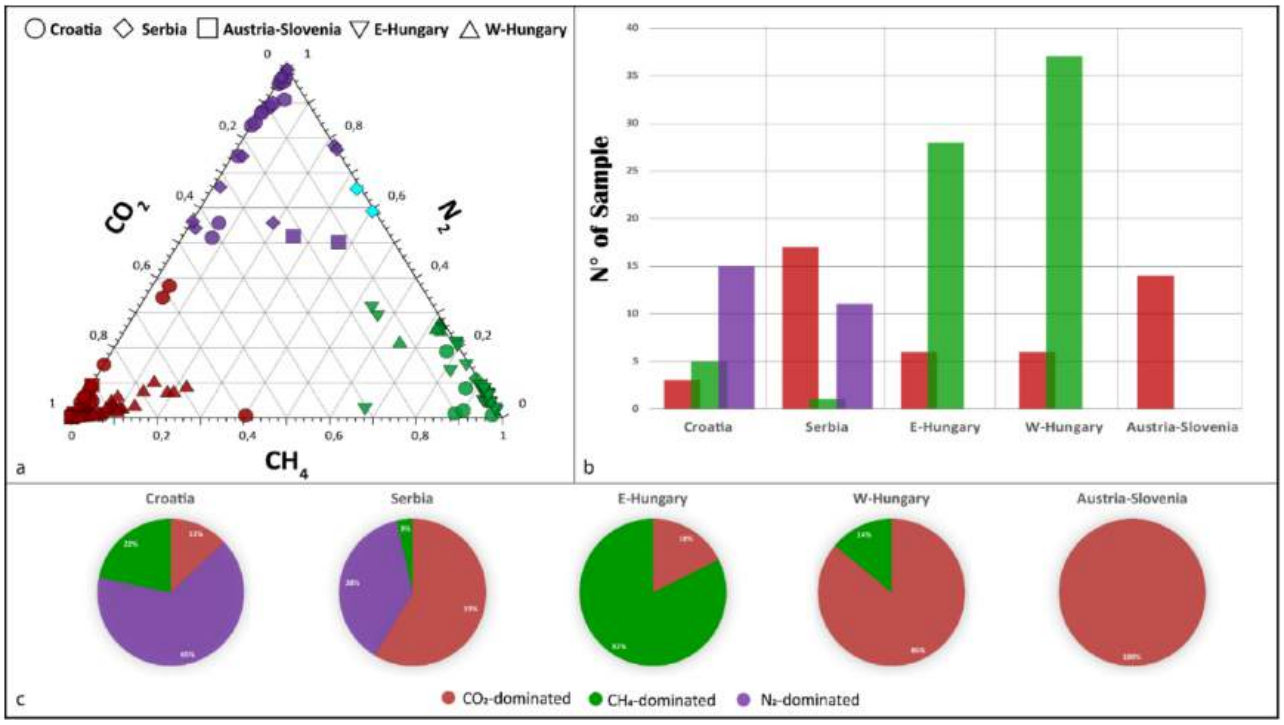

Fig. 3. a) Ternary diagram showing the chemical composition of the samples; b) Bar diagram and pie chart showing the distribution of samples, based on chemical composition, between the different regions.

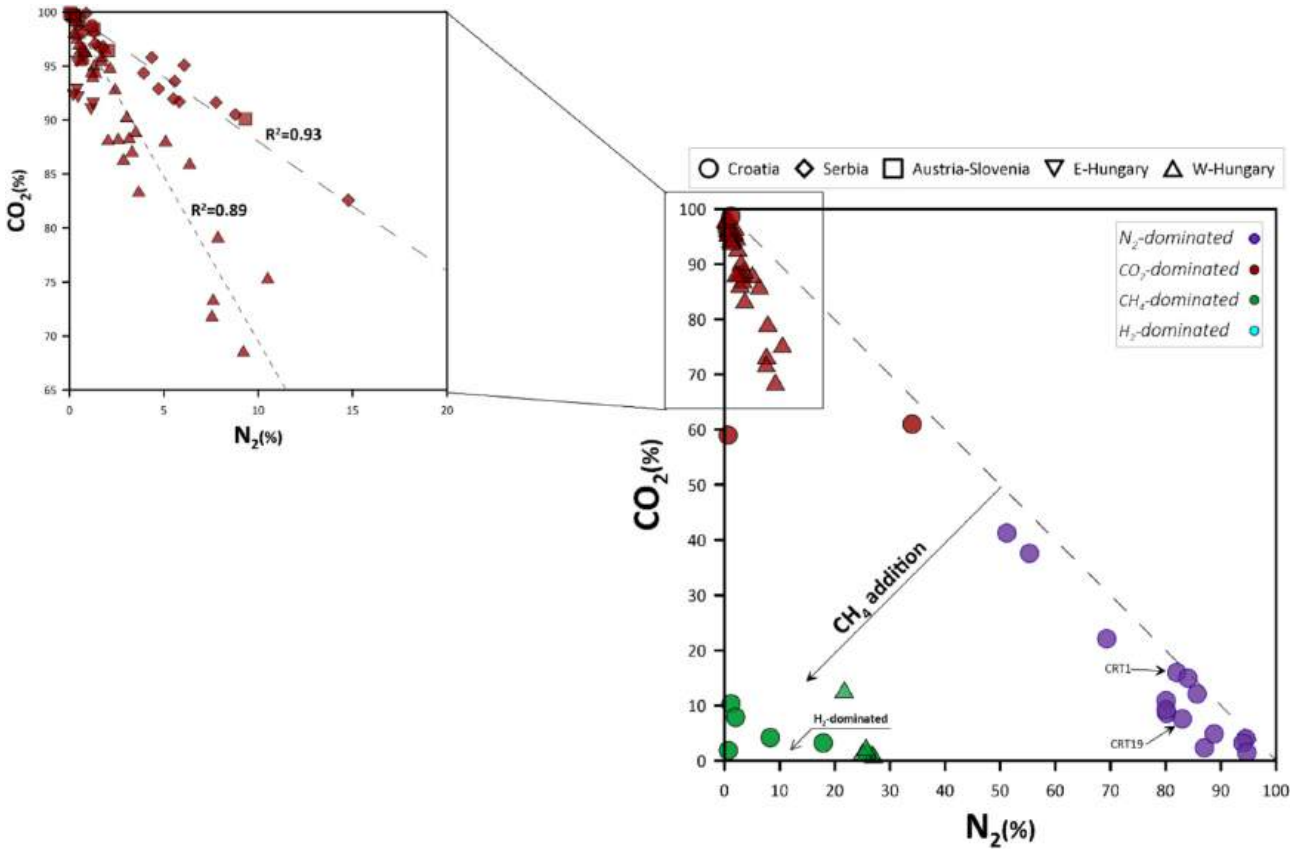

Fig. 4. N_2 vs. CO_2 concentrations plot. N_2 and CO_2 concentrations exhibit a negative correlation with clear mixing lines defined by linear regression. The mixing lines show the same CO_2 end-member (i.e 100 %) but different N_2 end-member. Line with $R^2 = 0,93$ refers to a 100 % N_2 end-member while line with $R^2 = 0,89$ refers to N2 end-member <15 %. The zoomed area shows some CO_2-dominated samples plotting along this latter mixing line. The other samples exhibit a prevailing CH4 composition and fall in the corner of the diagram, outside every mixing trend. Different symbols identify different areas, while different colors identify different chemical families, as already shown in Figs. 2 and 3 (see legend). CRT1 and CRT 19 are the samples collected outside the Pannonian basin region.

3.2.2. Helium

Helium in natural fluids is derived from three main sources, each characterized by different isotopic signatures: the continental mantle ($^3He/^4He = 8.2–9.3 \times 10^{-6}$), the crust ($^3He/^4He = 1.4–2.8 \times 10^{-8}$) and the atmosphere ($^3He/^4He = 1{,}4 \pm 0.005 \times 10^{-6}$) (e.g., Ballentine and Burnard, 2002; Ozima and Podosek, 2002). ^3He is primarily of primordial origin, trapped in the mantle since the Earth's early formation, while He in the crust is predominantly radiogenic (^4He), produced by the α-decay of $^{235,238}U$ and ^{232}Th (e.g., Ballentine and Burnard, 2002). The isotopic signatures of He normalized to atmospheric value (Ra) are: (a) 6.32 ± 0.39 Ra for the European Subcontinental Lithospheric Mantle (ESCLM) (Gautheron et al., 2005), (b) 0.01–0.02 Ra for crustal fluids (e.g., Ballentine and Burnard, 2002), and (c) 1 Ra for air (Ozima and Podosek, 2002).

The He isotopic signature of gas samples from PB and adjacent regions range from 0.07 Ra to 6.32 Ra and hence is suggestives of mixtures of distinct pristine He components (atmosphere-crust-mantle). Considering the differences in the He isotopic composition and $^4He/^{20}Ne$ ratios between the three different He components ($^4He/^{20}Ne > 1000$ for crust and mantle, and 0.318 for air), it is possible to resolve their relative contributions by using the mixing equations proposed by Sano et al. (1997). We find the atmospheric contribution in gases from the study area to be ≤15 % (literature and new data; Fig. 5 and Table S1). In general, the lowest $^4He/^{20}Ne$ ratios (more air-like) are observed in the N_2-dominated samples, particularly in the Croatian samples. These have $^4He/^{20}Ne$ ratios from 3 to 133 that, although suggestive of some more substantial air contribution, are still one order of magnitude higher than the same ratio in air (0.318), so the atmospheric component in these gases remains very low. The highest $^4He/^{20}Ne$ (≥ 3000) ratios are exhibited by CH_4 and CO_2-dominated samples from wells in Hungarian hydrocarbon fields. The correlation between N_2-dominated samples and the lowest $^4He/^{20}Ne$ values could indicate a shallow (atmospheric) source for these samples (see paragraph S2 in supplementary materials). The mantle contribution is estimated to vary between 1 and 50 % in the majority of the samples (Fig. 6). Only the gas samples from the Austria-Slovenia sector (Bräuer et al., 2016) and some samples from W-Hungary (Palcsu et al., 2014), exceed this value (e.g. Br2 = 100 %; Mihályi M25 = 65.6 %). On the other hand, lower (< 1 %) mantle contributions are inferred from the compositions of two Croatian N_2-rich samples (CRT1 and CRT19, 0.02 and 0.05 R/Ra, respectively. Fig. 1 and Fig. 5).

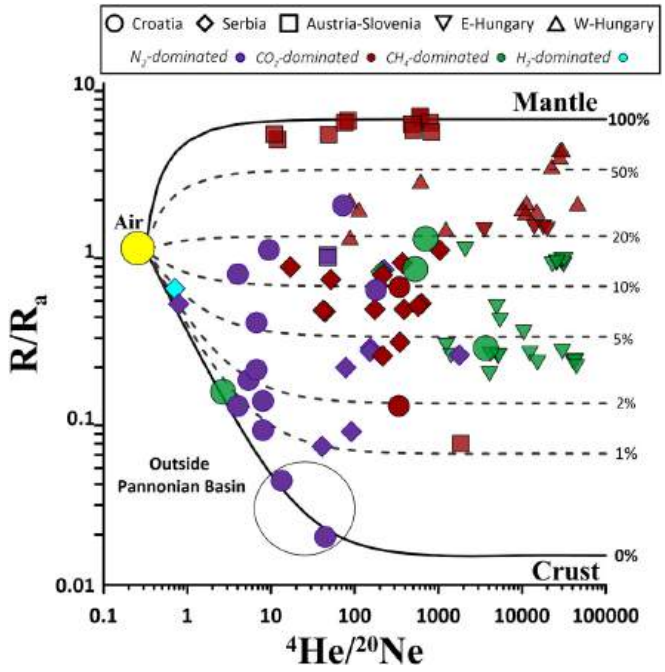

Fig. 5. He isotopic composition (expressed as R/R_a) versus $^4He/^{20}Ne$ ratios. The highest atmospheric contamination is shown by Croatian N_2-dominated samples ($^4He/^{20}Ne \geq 10$) and by H_2-dominated (SRB16/B) and other N_2-dominated sample with relative high H_2 concentration (34 %; SRB17/A) from Serbia region. Mantle contribution spans over a wide range from 1 % up to 50 % with a mean value of 22 % (see Fig. S10). Higher contributions (>50 %) are showed by some CO_2-dominated free gas samples from Austria-Slovenia border, while typical crustal values (0.02 and 0.05 Ra) are showed by N_2-rich samples collected outside the Pannonian basin region (inside the black circle).

4. He—C relationships

CO_2 sources and sinks during fluids migration through (and storage within) the crust are investigated by combining the amounts of He and CO_2 and their isotopic signatures in fluid emerging at the earth's surface in the PB (e.g., Randazzo et al., 2021, 2022; Barry et al., 2020; Holland and Gilfillan, 2013; Sano and Marty, 1995). The amount of CO_2 and its carbon isotopic composition in geogenic fluids can result from five main processes: 1) mixing of gases from different sources; 2) partial gas dissolution in groundwater; 3) degassing from water; 4) C-bearing mineral phases precipitation; and 5) oil biodegradation/methanogenesis. In this contest, the C—He systematic is useful for evaluating enrichments or depletions relative to their sources (e.g., the mantle-like signature) and how the carbon isotopic signature of CO_2 is modified by these processes. Here, we assume a $CO_2/^3He$ ratio of 2–7 × 10^9 and $\delta^{13}C_{(CO2)} = -3.5$ ‰ as representative of the mantle below the PB (Rizzo et al., 2018; Bräuer et al., 2016). These mantle values are slightly different from the typical MORB mantle (e.g., $CO_2/^3He = 1.5–2 \times 10^9$, Marty et al., 2020) because, in continental setting, the lithospheric mantle often brings record of heterogeneities caused by deep processes such as subduction and/or metasomatism that can lead to carbon enrichment or, in general, a modification of its chemical composition (e.g Rizzo et al., 2018). We find that the $CO_2/^3He$ ratios in the PB gas samples are either higher (up to 5.3×10^{11}) or lower (as low as 3.3×10^5) than the inferred mantle range (from Fig. 6 to Fig. 10). Here, we investigate each of the aforementioned processes that can affect $C/^3He$ and $\delta^{13}C_{CO2}$ to figure out their effect, at regional scale, on the PB's natural fluids escaping into the atmosphere.

4.1. Mixing

Mixing is a first-order process that could affect the amounts and isotopic composition of the different gaseous species emitted in the atmosphere. During the transfer through the crust, mantle-derived gases can mix with crustal fluids originating from different sources and the resulting fluids take memory of this process. According to previous large-scale geochemical investigations (e.g., Sano and Marty, 1995; Sherwood et al., 1997), values higher than mantle $CO_2/^3He$ ratios can be interpreted as due to the addition of crustal-derived CO_2, produced by decarbonation reactions and/or biological processes.

According to the approach proposed by Sano and Marty (1995), which is based on three-components mixing equations, it is possible to deconvolve mantle and crustal carbon fractions using the $CO_2/^3He$ ratio and $\delta^{13}C$ of CO_2 because the different sources are characterized by specific $CO_2/^3He$ ratios and $\delta^{13}C$ values. Assuming a mantle end member with $CO_2/^3He$ of 2–7 × 10^9 and $\delta^{13}C_{(CO2)} = -3.5$ ‰ (Bräuer et al., 2016; Rizzo et al., 2018) and three crustal-sourced end-members with $CO_2/^3He$ ratio of 10^{13} and $\delta^{13}C$ of 0 ‰, −30 ‰ and + 20 ‰ for limestone, biogenic and hydrocarbon biodegradation, respectively (Sano and Marty, 1995; Milkov, 2020), we solve the contribution of the different pristine sources contributing to the fluids in the PB (Fig. 8–9-10). Therefore, some CO_2-dominated gases from Serbia and *E*-Hungary could simply be the result of mixing between a mantle component and limestone-derived fluids with a low contribution from biogenic sources. In fact, these gases do not lie exactly along the mixing line between the mantle and the limestone components. However, we cannot rule out the

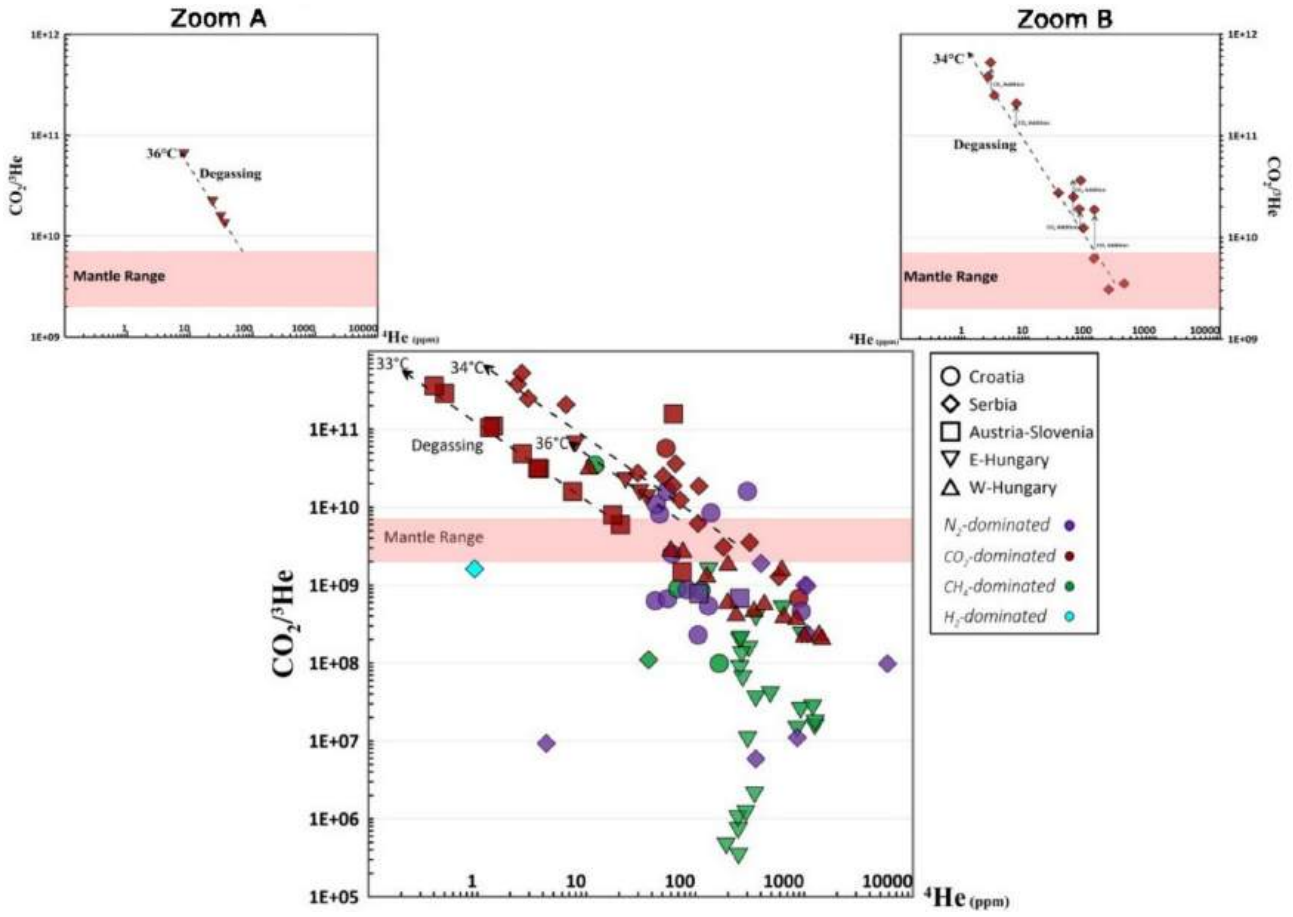

Fig. 6. $CO_2/^3He$ ratios versus ^4He. The panel shows a decreasing $CO_2/^3He$ trend with increasing ^4He. The shaded area represents the SCLM range ($2–7 \times 10^9$; Bräuer et al., 2016; Marty et al., 2020). Black dotted arrows are the degassing trend. Zoom A = Serbia samples; Zoom B *E*-Hungary samples. The temperatures shown are the average for every area. Here, we assumed a salinity of 0 ‰. See Section 4 for more details.

hypothesis that these gases also contain contributions from the biodegradation component. The latter assumption is certainly valid for samples CRT7 and CRT8, which exhibit the highest $\delta^{13}C$ values (+12.8 and 10.6 ‰), suggesting a mixing between a mantle component and a dominant component linked to oil biodegradation (Fig. 8–9). In addition, the four Croatian N_2-dominated samples (CRT1-CRT12-CRT18-CRT19) can be linked to mixing between mantle-derived and biogenic-derived fluids (Fig. 8).

4.2. Degassing

The release (i.e., degassing) of volatiles dissolved in groundwater is a process that can affect both the amount of CO_2 in natural fluids escaping to the surface and its carbon isotopic composition. This process causes the C-isotopes fractionation between gaseous CO_2 and various dissolved carbon species (i.e., HCO_3^-, CO_3^{2-}, H_2CO_3; Zhang et al., 1995). Here, we modeled the variability of both the $CO_2/^3He$ ratio and $\delta^{13}C_{(CO2)}$ in gases escaping from groundwater by using a classical model of open-system degassing (e.g., Hiett et al., 2021; Buttitta et al., 2023; black arrows in Fig. 6 and 7 and blue arrow in Fig. 8; see section S4.2 in supplementary materials for more details).

As shown in Fig. 6, while the CO_2-dominated samples from *E*-Hungary fit the trend, a few Serbian samples deviate from it (zoom B in Fig. 6), suggesting that more than one process can contribute to the variability in $CO_2/^3He$ ratios (i.e., degassing + crustal CO_2 addition).

Moreover, the E-Hungary and Serbia CO_2-dominated samples also deviate from the trend shown in Fig. 8 (blue arrow). This suggests the predominance of mixing processes over degassing processes, which, in addition to increasing $CO_2/^3He$ ratios, generate an increase in $\delta^{13}C_{CO2}$ (shifting the values to the right side in Fig. 8).

On the other hand, the mixing processes cannot explain the composition of the gases emitted in the Austria-Slovenia area because, despite having $CO_2/^3He$ ratios higher than typical mantle values (Fig. 6, 7 and 8), these samples show typical mantle-like He isotope ratios (Fig. 7). Indeed, in the case of mixing with a crustal-derived CO_2, the He isotopic ratio should shift toward lower values (i.e., crustal values) following the mixing lines of Fig. 7. So, excluding an additional crustal CO_2 contribution to the mantle component, the low He concentration (from 1 to ~10 ppm) coupled with the high $CO_2/^3He$ ratios (up to 10^{11}) can be explained by solubility-dependent fractionation between gas and water at shallow depths, which causes He leak (e.g., Bräuer et al., 2016; Randazzo et al., 2021).

The good fit of Austria-Slovenia samples with our degassing model in Figs. 6 and 7 suggests that the relative abundance of CO_2 and He can be explained by volatile loss from the water due to gas oversaturation at the fixed conditions. Moreover, as shown from Fig. 8, the CO_2-dominated samples from Austria-Slovenia fit the degassing trend better than those from Serbia and E-Hungary. This suggests the predominance of degassing processes in modifying the $CO_2/^3He$ ratio for these samples. However, even for these samples, concomitant mixing processes between different sources (e.g., a biogenic source) cannot be ruled out.

4.3. Gas dissolution

In a system where the uprising volatiles partially dissolve in groundwater, CO_2 dissolves preferentially in water compared to He due

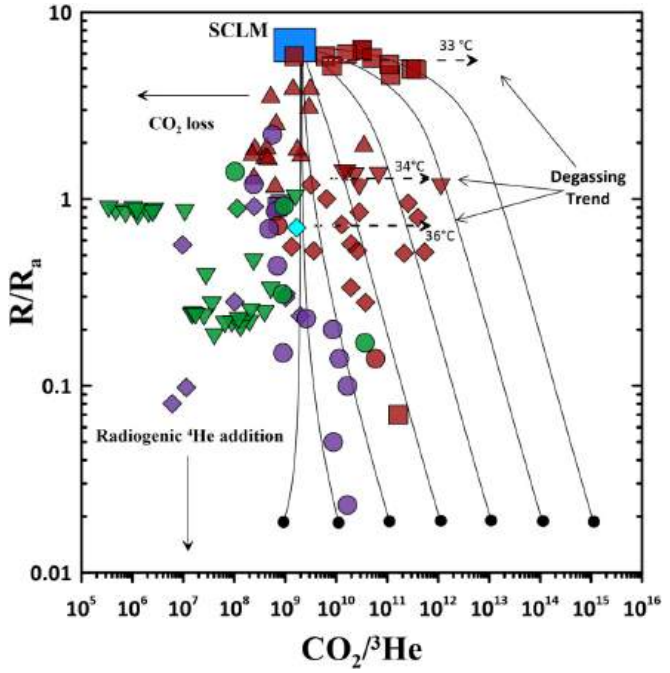

Fig. 7. $^{3}He/^{4}He$ (expressed as R/Ra) versus $CO_2/^{3}He$ ratio plot. Binary mixing curves are shown between the SCLM (6.1 ± 0.9 Ra and $CO_2/^{3}He$ of 7 × 10^9; Bräuer et al., 2016; Gautheron and Moreira, 2002) and different hypothetical crustal end-members with the same helium isotopic composition (0.02 Ra) but variable $CO_2/^{3}He$ ratios. Black dotted arrows show the same degassing trends of Fig. 6.

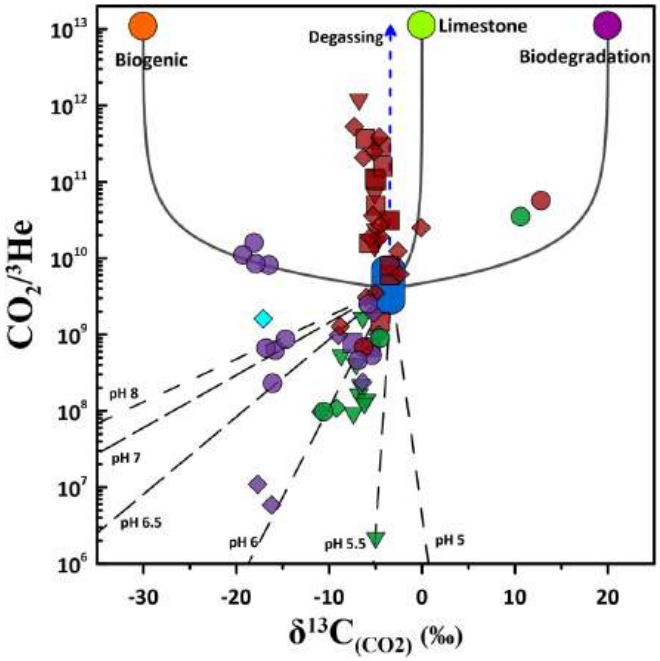

Fig. 8. $CO_2/^{3}He$ versus $\delta^{13}C(CO_2)$ plot. Dashed lines show the predicted model for Rayleigh-type gas dissolution at salinity 0 ‰ and 25 °C. The model curves (dashed lines) are obtained over a range of pH values for increasing extents of gas dissolution. Solid lines show mixing trends between mantle end-member with $CO_2/^{3}He$ = 2–7 × 10^9 and $\delta^{13}C$ = −3.5 ‰ (Bräuer et al., 2016; Rizzo et al., 2018), limestone ($CO_2/^{3}He = 10^{13}$, $\delta^{13}C$ = 0 ‰), sediment ($CO_2/^{3}He$ = 1 × 10^{13}, $\delta^{13}C$ = −30 ‰) and hydrocarbon/oil biodegradation ($CO_2/^{3}He$ = 1 × 10^{13}, $\delta^{13}C$ = 20 ‰; Milkov, 2020). After Sano and Marty (1995). The blue arrow shows the degassing trend computed at a temperature of 34 °C (i.e., the average T of our samples that exceed the mantle $CO_2/^{3}He$ ratio). See section 4 in supplementary materials for equations and details. (For interpretation of the references to colour in this figure legend, the reader is referred to the web version of this article.)

to its higher solubility (at temperatures up to 90 °C: Ballentine et al., 2001).

In the PB, two main groundwater flow regimes have been recognized at a regional scale (Erdelyi, 1976; Ottlik et al., 1981; Horváth et al., 2015 and reference therein): (i) a shallow system that is recharged by meteoric water at topographic highs and discharges at topographic lows, and (ii) a deeper groundwater circulation with high-salinity water within the Pliocene and Miocene sediments, locally connected to the shallower systems (Ballentine et al., 1991; Tóth and Almási, 2001). Hence, in accordance with these two scenarios, to model the gas-water interaction as partially dissolution of gas in water, we consider two end-member conditions: 1) a low salinity (S) water reservoir (S = 0 ‰), and 2) a salt-rich water reservoir (S = 35 ‰). Here, we assume a partial dissolution process modeled as open-system (Rayleigh type) degassing (e.g., Gilfillan et al., 2009; Randazzo et al., 2021). Assuming a mantle-like composition typical of the SCLM for the pristine gas ($CO_2/^{3}He$ = 2–7 × 10^9, $\delta^{13}C$ = −3.5 ‰; Bräuer et al., 2016; Marty et al., 2020; Rizzo et al., 2018), we modeled the progressive variation of the $CO_2/^{3}He$ ratio in the residual gas that moves through the water column and progressively dissolves in the water (Fig. 8). We stress that here we consider the case of a pristine gas as the mantle end-member, which can be modified by gas-water interactions under different conditions (25 °C < *T* < 100 °C, 5 < pH <8 and 0 ‰ < S < 35 ‰).

However, assuming a different end-member resulting from the mixing between crustal (limestone-organic/biogenic -biodegradation) and the mantle components (corresponding to each point within the large mixing field between the three endmembers in the $CO_2/^{3}He$ vs $\delta^{13}C_{(CO2)}$ diagram, Fig. 8), the degassing trends start within the area corresponding to different percentages of mixing (Randazzo et al., 2022). Overall, this model of partial CO_2 dissolution in water at pH between 5 and 8, *T* = 25C° and S = 0 ‰ fits the data that are characterized by $CO_2/^{3}He$ ratios lower than the mantle values, highlighting that part of the gases in the PB region can be representative of different degrees of CO_2 loss by dissolution in water (up to 90 %). Therefore, the water-gas interactions can reasonably explain the $CO_2/^{3}He$ vs. $\delta^{13}C$ relationships (Fig. S3 to S6 in Supplementary materials) at the regional scale over a large range of T (25–100 °C), S (0–35 ‰), and pH (5 to 8).

4.4. Calcite precipitation

Calcite precipitation from a CO_2-rich groundwater is an additional process that can decrease the $CO_2/^{3}He$ ratios and, at the same time, fractionate $\delta^{13}C_{CO2}$ (e.g. Gilfillan et al., 2009; Barry et al., 2019; Randazzo et al., 2021, 2022). Once CO_2 is dissolved into groundwater, it can react with ions (e.g., Na^+, Ca^{2+}, Mg^{2+}) to precipitate carbonate minerals, leading to both lower $CO_2/^{3}He$ ratios and more negative $\delta^{13}C$ values in residual gases (Barry et al., 2020). Following Buttitta et al., 2023, we calculate the changes in $CO_2/^{3}He$ and $\delta^{13}C_{CO2}$ predicted for CO_2 precipitation in carbonate at different water conditions (i.e., pH, T, and salinity; Fig. 9a and b). The modeled curves only partially fit the composition of the natural fluids (Fig. 9 a, b, Figs. S7 and S8 in supplementary materials). Even though a significant number of data points are not consistent with carbonate precipitation, we cannot rule out the possibility that this process locally affects the chemical and isotopic composition ($\delta^{13}C$) of gases in the PB.

4.5. Methanogenesis

In crustal layers, groundwater can also play an active role in methane generation, bringing microbes to isolated or sterilized subsurface environments (Zhou et al., 2005 and references therein). Microbial methanogenesis occurs in a wide range of environments (Heuer et al., 2020;

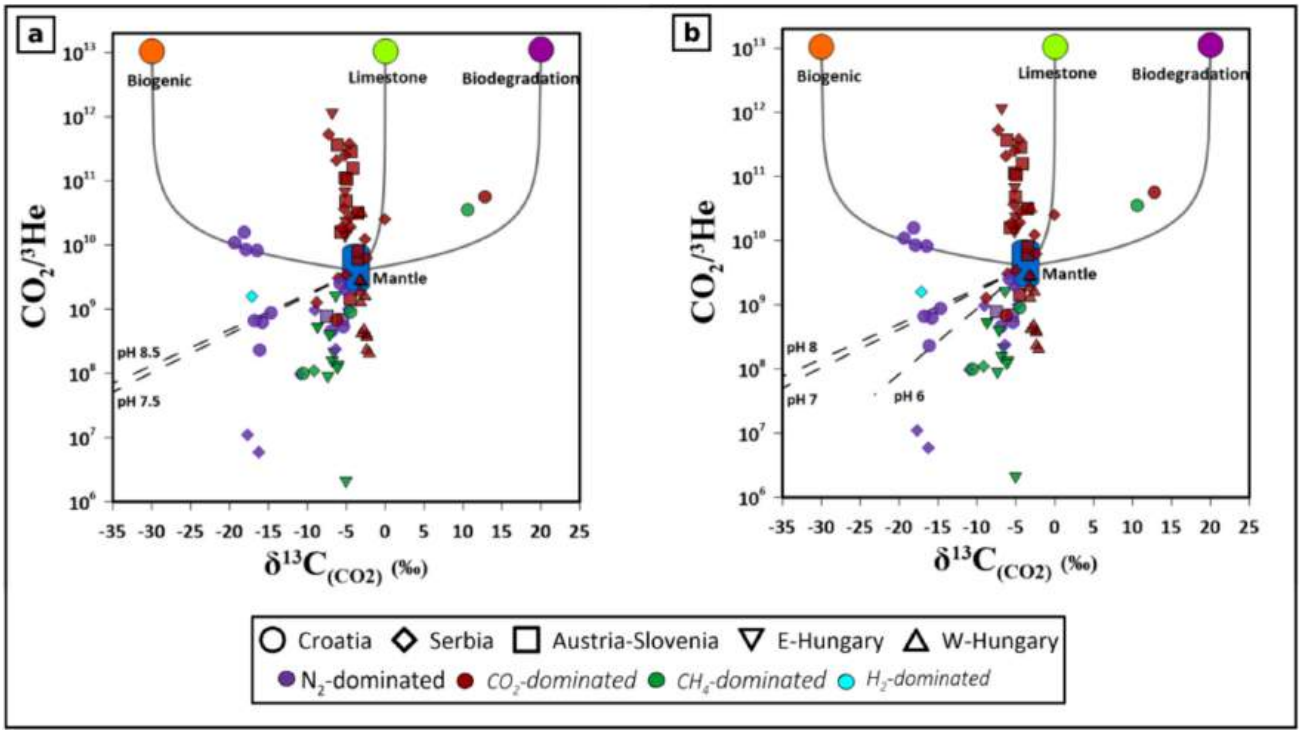

Fig. 9. $CO_2/^3He$ versus $\delta^{13}C(CO_2)$ plot. Dashed lines represent the predicted trends for carbonate mineral precipitation at 25° and a) salinity 0 ‰, b) salinity 35 ‰. In the case of precipitation there is zero ^3He loss from the CO_2 phase and $CO_2/^3He$ changes in proportion to the fraction of the remaining CO_2 phase. The carbonate-water equilibrium is temperature, pH and P_{CO2} dependent. From these parameters depend the abundance of each carbon species and the pHs at which carbonate precipitation can occur in the system. Equations from Buttitta et al., 2023 and Gilfillan et al., 2009.

McIntosh et al., 2010; Conrad, 2005) through two principal pathways: 1) hydrogenotrophic methanogenesis (also called the "carbonate reduction" pathway), which can be represented by the general reaction: $CO_2 + 4H_2 \rightarrow CH_4 + 2H_2O$, and 2) acetoclastic methanogenesis, where microbes can generate methane from the consumption of acetate (i.e., organic acids derived from organic matter) according to the following reaction: $CH_3COOH = CH_4 + CO_2$ (Whiticar, 1999). In addition to the relatively well-documented acetoclastic and hydrogenotrophic pathways, recent studies have also identified the importance of methanogenesis utilizing a range of methylated compounds (Vinson et al., 2019 and references therein). In fact, at temperatures lower than ~120 °C (the upper temperature limit for methanogens), almost all rock environments contain microbes in water-filled pore spaces and fractures (Takai et al., 2008). Besides temperature, salinity represents an additional key-parameter affecting microbial growth and methanogenic biodegradation (Baek et al., 2019; Reeve et al., 1997). Numerous studies have identified hydrogenotrophic methanogens in some oil fields and in reservoirs hosting hydrocarbons where CO_2 has been converted to CH_4, including some within the PB (e.g. Tyne et al., 2023 and references therein). In fact, Sherwood et al. (1997) discussed CO_2 conversion to CH_4 within the Szegholm Gas Field in the PB (*E*-Hungary). Moreover, the conversion of CO_2 to CH_4 through methanogenesis has been identified as a potential carbon trapping mechanism by Tyne et al. (2021) for some of these hydrocarbon reservoirs in the PB (Szegholm South Gas Field). Here, we explored whether the same processes could explain the chemical variability in other hydrocarbon fields in both western and eastern Hungary. In fact, these fluids also show geochemical signatures consistent with the possible occurrence of methanogenesis at depth (e.g., Szegholm North, Ebes, Hajduszoboszlo, Kismarja and Repcelak gas fields. See Table S1 and references therein). Here, we summarize the main conclusions from previous investigations (i.e. Tyne et al., 2021 and references therein) regarding the origin of CH_4 in the PB, which is useful for the discussion about CH_4. The C and H isotopic composition of CH_4 indicated its thermogenic origin with moderate maturation level for the W-Hungary samples (Palcsu et al., 2014). For the E-Hungary Hydrocarbon field samples, Tyne et al. (2021) proposed that the presence of biogenic CH_4 (through CO_2 conversion) can be clearly identified from the measured C_1/C_N in the Szegholm South Gas Field (0.946 ± 0.004; Sherwood et al., 1997), which is greater than what would be expected in a purely thermogenic system (0.909). Based on this, the samples from W-Hungary hydrocarbon fields can also be considered interesting with respect to microbial methanogenesis since they show a C_1/C_N ratio one order of magnitude greater than that of the Szegholm South Gas Field (Palcsu et al., 2014).

Considering the inferences by Tyne et al. (2021), a small portion of the methane present in the Hungarian hydrocarbon fields could therefore be biogenic in origin in the Hungarian part of the PB. In particular, we observed that water-gas interaction and carbonate-minerals precipitation can occur at depth and are concomitant processes for CO_2 removal from the deep fluids within the crust in the PB (Figs., 8 and 9), which is a pre-requisite for microbial hydrogenotrophic methanogenesis (Tyne et al., 2023). Moreover, the estimated temperatures for these fields are between 40 °C and 105 °C (Horváth et al., 2015 and references therein), so within the range of microbially driven methanogenesis. Therefore, we used a simple model of methanogenesis–dissolution to explore a possible effect of these processes on the carbon and its isotopic composition in the Hungarian PB area (Fig. 10), as previous geochemical investigations proposed at the local scale in the PB. In fact, according to Tyne et al. (2021), a dissolution process (at pH 7) and methanogenesis processes control the abundances of CO_2 and He at regional scale in the E-Hungary sector of the PB, at least in those fluids that are characterized by $C/^3He$ lower than the mantle value ($CO_2/^3He = 2–7 \times 10^9$). Here, we find that Hungarian gases can be explained by the combination of processes such as microbial methanogenesis and dissolution (Fig. 10). Within this hypothesis, methanogenesis increases from W-Hungary samples, which show almost pure dissolution as process of CO_2 removal, to E-Hungary samples, as indicated by Methanogenesis-Dissolution ratio (M:D). The M:D ratio varies from 0.02 for the sample least affected by

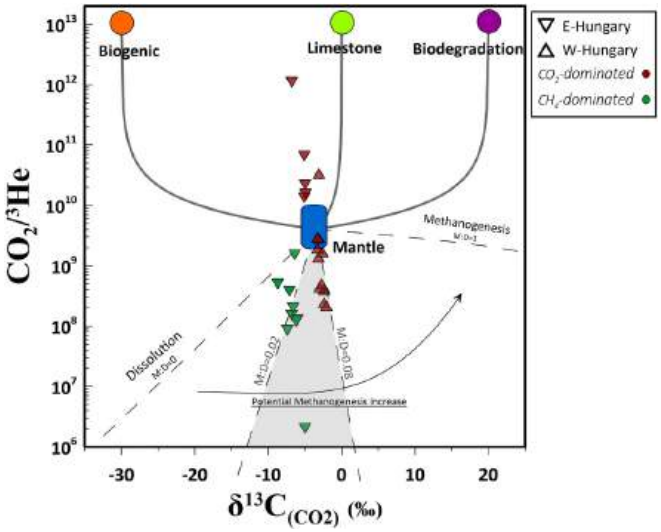

Fig. 10. $CO_2/^3He$ ratio as a function of the $\delta^{13}C$ of CO_2 in the East and West Hungary gas samples at the average T of 75 °C and pH value of 7. Dashed lines show end-member methanogenesis and dissolution fractionation trajectories. The shaded region represents trapping by the combination of microbial methanogenesis and dissolution. Methanogenesis increases from left to right. The upper and lower methanogenesis: dissolution ratios (M:D) are 0.02 and 0.08, respectively, showing that dissolution is the dominant processes with respect to microbial methanogenesis.

methanogenesis up to 0.08 (shaded area in Fig. 10). Therefore, methanogenesis may play a substantial role in the amount of CO_2 and its isotopic composition in PB shallow crustal gases.

In conclusion, we would like to emphasize that the occurrence of different concomitant processes plays an active role in the chemistry (chemical and isotopic composition) of the volatiles at depth. In fact, different conditions can occur at depth and, for a crustal sector with a potentially high number of stratified aquifers, such as in the PB, a simple open-system (Rayleigh type) degassing model is evidently too simplified. In fact, it cannot be ruled out that more complex gas-aquifer interactions, such as complete gas dissolution in deep aquifer, followed by multistep degassing upon groundwater upward migration (Chiodini et al., 2011), could have taken place. This notwithstanding, our model clearly highlights the role played by gas-water-rock interactions in modifying the composition of the studied gas manifestations.

5. Mantle degassing and tectonic implications

The Pannonian Basin exhibits a complex geochemical and geodynamic framework, with mantle-derived volatiles providing evidence of deep mantle contributions in various sectors of the PB region. Based on geological and geochemical evidence, three different sources of mantle volatiles are thought to coexist in the different areas within the PB: (i) Fossil mantle-derived gases have been identified in hydrocarbon fields in East and West Hungary. These gases were likely released by Neogene magmatic intrusions and migrated through tectonic structures (Ballentine et al., 1991; Palcsu et al., 2014); (ii) Recent magmatic intrusions drive mantle degassing in the Austria-Slovenia region, where mantle volatiles ascend along tectonic discontinuities, suggesting an underlying active magmatic reservoir that facilitates the release of mantle-derived fluids (Bräuer et al., 2016); (iii) in Serbia, asthenospheric ascent is linked to high heat flows and direct release of mantle volatiles, with little evidences of fossil gas contributions (Randazzo et al., 2021; Belinić et al., 2021). Similarly, thermal anomalies in Croatia (Hurter and Haenel, 2002; Živković et al., 2016) are unlikely to be explained by fossil mantle gases alone, thus requiring recent mantle input or magmatic intrusions. Fault systems play a critical role in transporting mantle volatiles, with intraplate seismicity and deep earthquakes confirming crust-mantle connections (Markušić, 2008, Markušić et al., 2021). However, the available data do not allow for a complete distinction between these sources at regional scale, as overlapping processes and complex subsurface interactions may contribute to the observed volatile signatures. This is further supported by the intricate interplay of mantle dynamics, tectonic activity, and lithospheric processes in the PB.

Assuming these potential contributions of mantle He in the PB, we approached a quantitative mantle-He flux estimation to provide insights into 1) the rate of volatile transfer through the crust, and 2) the tectonic regime at regional scale (e.g. Ballentine et al., 1996). O'Nions and Oxburgh (1988) proposed a method to assess the flux of mantle-derived He in continental regions far from volcanism, which they applied to the PB. This approach assumed that if He degassing occurs at a steady state, the mantle He flux can be estimated from the He isotope composition of the system. This estimation requires an initial assessment of the crustal He flux range and considers that the addition of crustal radiogenic ^4He, during the transfer of mantle-derived fluids through the crust, produces a decrease of the pristine mantle He isotopic ratio. Since their study, new geochemical datasets, including those analyzed in this work, allow for more accurate estimates of mantle He fluxes in the PB. Our updated estimates range from 10^9 to 10^{11} atoms m^{-2} s^{-1} (average values in Fig. 11c; see details in Supplementary Materials, Section S5) which are up to three orders of magnitude higher than those typically observed in stable continental areas (~10^7 atoms m^{-2} s^{-1}; O'Nions and Oxburgh, 1988). Specifically, excluding outliers from the Croatian Pannonian area (samples CRT1 and CRT19), we estimate a mantle He flux for the PB of 1.7×10^{10} atoms m^{-2} s^{-1} (Fig. 11c), which is approximately one order of magnitude higher than previous estimates (3.7×10^9 atoms m^{-2} s^{-1}; O'Nions and Oxburgh, 1988). In tectonically active regions, crustal He release rates may reach values up to 10^4 times the steady-state flux due to stress-induced fracturing (Buttitta et al., 2020; Torgersen, 2010 and references therein). Additionally, low-magnitude earthquakes ($M < 4$) can cause impulsive increases in crustal He output, thereby enhancing the release of ^4He from rocks (Caracausi et al., 2022). Assuming a crustal ^4He flux from 10 to 10^4 times the steady-state value, the estimated mantle He fluxes increase to 10^{11}–10^{14} atoms m^{-2} s^{-1}, comparable to fluxes observed in active tectonic and volcanic systems (Fig. 11). We then calculated the mantle-derived ^3He flux, which ranges from 3.9×10^4 to 3.9×10^6 atoms m^{-2} s^{-1}. For the PB area (~5×10^4 km^2), this corresponds to a total flux of 0.10–10 mol ^3He yr^{-1}. Using the same parameters as Ballentine et al. (1996) (see Secton 5 in supplementary materials) our ^3He flux values imply a productive melt volume of 2.6×10^{-3} to 4.3×10^{-1} km^3 yr^{-1}, which is up to three orders of magnitude higher than the volume estimated by Ballentine et al. (1996).

The combination of available $CO_2/^3He$ ratios, R/Ra values, and mantle He fluxes allows us to estimate mantle CO_2 fluxes in the PB region. These values range from 10^3 to 10^5 mol·km^{-2}·yr^{-1} (Fig. 11d), consistent with fluxes reported for volcanic and tectonically active regions worldwide (Caracausi and Paternoster, 2015; Foley and Fischer, 2017). Examples include the African Rift system (up to 2.5×10^5 mol·km^{-2}·yr^{-1}; Foley and Fischer, 2017), regional CO_2 degassing structures in central ($3.7–4.7 \times 10^6$ mol·km^{-2}·yr^{-1} Chiodini et al., 2000; Chiodini et al., 2021a, 2021b; Frondini et al., 2018) and southern Italy (i.e. Irpinia and Calabria region; Buttitta et al., 2023, Randazzo et al., 2022) and the San Andreas Fault (4.0×10^4 mol·km^{-2}·year; Kulongosky et al., 2013). Although these flux estimates are approximate and require further refinement, they represent the first quantitative assessment of CO_2 fluxes for the PB region. Taken together with evidences of extensional tectonics (Faccenna et al., 2014), active seismicity (Markušić et al., 2021), elevated heat flows (up to 130 mW m^{-2}; Horváth et al., 2015), and lithospheric discontinuities (Brückl et al., 2010), our results suggest that the release of fluids and heat in the PB region is linked to mantle-derived processes and associated magmas.

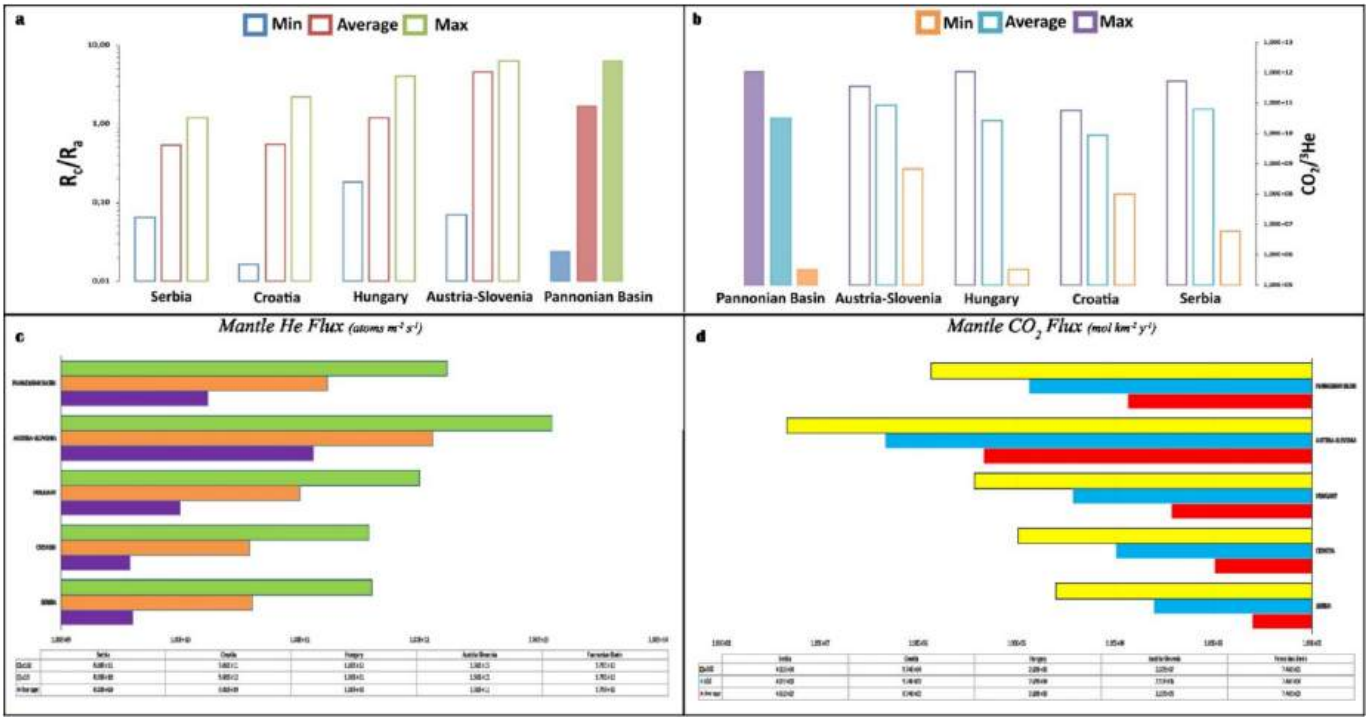

Fig. 11. a) Minimum, Average and Maximum value of R_c/R_a for each region and for PB area*; b) Minimum, Average and Maximum value of $CO_2/^3He$ ratio for each region and for PB area*; d) Mantle He fluxes estimated for each region and for PB area*; e) Mantle CO_2 fluxes** estimated for each region and for PB area*.
*PB area is the sum of Croatia, Hungary and Austria-Slovenia region. Average values are defined by considering the set of values from these regions. Purple = average value; Orange = 10× the average value; Green = 100× the average value.
** Average $CO_2/^3He$ values were defined by considering for each region only the values falling within the mantle range. For the PB area we considered the $CO_2/^3He$ within the mantle range of the regions previously mentioned. Red = average value; Blue = 10× the average value; Yellow = 100× the average value. (For interpretation of the references to colour in this figure legend, the reader is referred to the web version of this article.)

6. Summary and future perspectives

This work reports the first comprehensive geochemical dataset on gas manifestations for the Croatian Pannonian basin area, along with a detailed geochemical review of various natural manifestations within the PB system and the nearby Vardar zone region, with the aim to enhance our understanding of the processes that act during the upwelling and emplacement of fluids at shallow crustal depth, and their relationships with the underlying mantle and crustal structures. The main conclusions are:

1) The chemical and isotopic composition of natural gases is highly heterogeneous, clustering into three groups: N_2-dominated, CH_4-dominated, CO_2-dominated. The first group is mainly concentrated in the Croatian PB and Serbian Vardar zone. Two samples dominated by H_2 were identified in the Serbian Vardar zone.
2) For the first time, the He isotopic composition of samples from the Croatian part of the PB was analyzed and compared with the previous studies in nearby areas. Mantle contribution vary widely across the entire PB area, from 1 % up to 50 %. The highest contributions are observed in the Austria-Slovenia border area (up to 100 %; Bräuer et al., 2016) and W-Hungary (up to 65.58 %; Palcsu et al., 2014). Croatian N_2-rich samples collected outside the PB region (CRT1 and CRT19; Fig. 5 and S10) show lower values, less than 1 %.
3) Groundwater interactions, in variable extents, are inferred from atmosphere-derived noble gases. The computed gas-to-water volume ratios (Vg/Vw) range from 0.002 to 66, with the lowest values found in the N_2-dominated samples. The latter exhibit the highest ^{20}Ne concentrations, indicating greater involvement of groundwater and/or shallower origin compared to CO_2 and CH_4-dominated samples (see supplementary materials).
4) Based on their He and C isotope compositions, the samples with high $CO_2/^3He$ ratios (relative to the mantle value) are interpreted as mixtures of crustal CO_2-rich gases (from organic-biogenic sources) and mantle-derived components, and/or as being affected by degassing to different degrees. Furthermore, a few samples from Croatia show mixing between mantle components and CO_2 produced by oil biodegradation processes (see Section 3 in supplementary materials), thus evidencing that partial conversion of oil-derived CO_2 into secondary microbial methane occurs in crustal layers.
5) Processes of gas-water interaction are investigated to determine their influence on the chemical and isotopic composition of the gases in the PB. Most of the samples could be affected by extensive chemical and isotopic fractionation due to partial dissolution of gases in water and consequent loss of CO_2 during emplacement/migration in shallow crustal layers. The lost free-CO_2 fraction likely remains trapped at deep aquifer conditions in either dissolved or mineral form. Methanogenesis has also been investigated as a CO_2 loss mechanism, and although it is not the dominant process, it may play a role in trapping carbon within the crust.
6) Using the He isotopic composition, the mantle-derived He fluxes were estimated for each region and ranged from 10^9 to 10^{11} atoms m^{-2} s^{-1}, three orders of magnitude higher than normally found in stable continental areas. Averaging the He isotopic compositions of all PB samples, an average mantle He flux for the entire PB region, ranging from 1.7×10^{10} to 1.7×10^{12} atoms m^{-2} s^{-1}, is estimated. This value is one order of magnitude greater than that determined by O'Nions and Oxburgh (1988) and places the PB among the areas affected by strong tectonic stress and/or active volcanism, in line with the findings in neighboring areas, such as central and southern Serbia (Randazzo et al., 2021; Fig. 12). Moreover, these He flux values correspond to an estimated melt volume of 2.6×10^{-3}-4.3 ×

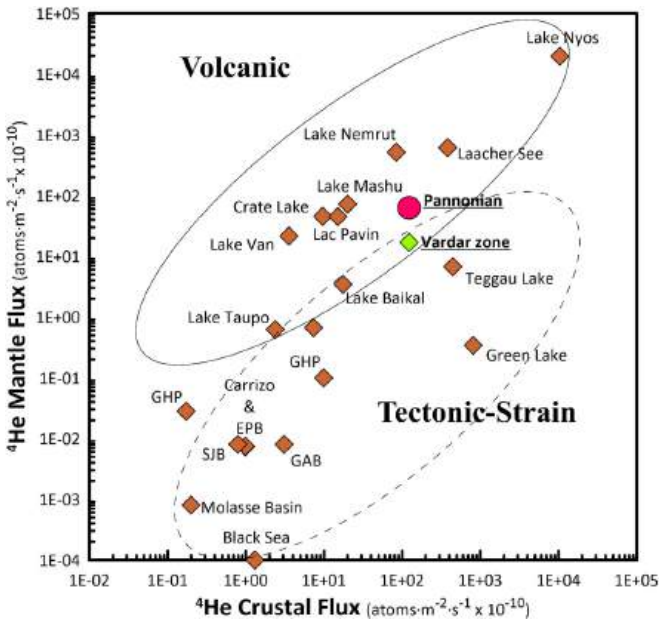

Fig. 12. Crustal-derived ^{4}He fluxes compared to mantle-derived ^{4}He fluxes. The assessed mantle-derived He flux for the PB is 1.5×10^9 atoms m^{-2} s^{-1} using the average He isotope composition (Rc/Ra) of gas from the different Pannonian basin areas. For crustal-derived ^{4}He fluxes being 10–10^4 times higher than the *"steady-state"* crustal flux, the mantle He fluxes would also be in the order of magnitude of values characteristic of "Volcanic field" and/or "Tectonic-strain field" (modified after Torgersen, 2010). The pink circle is the average value for the Pannonian basin region, while the green diamond is the value for the Serbian Vardar zone (Randazzo et al., 2021). Orange diamonds from Torgersen, 2010. (For interpretation of the references to colour in this figure legend, the reader is referred to the web version of this article.)

10^{-1} km^3 melt yr^{-1}, up to three orders or magnitude higher than the previous estimations (Ballentine et al., 1996).

7) The mantle-derived CO_2 fluxes for the PB area was also computed from the $CO_2/^3$He ratios, obtaining a range between 10^3 and 10^5 mol·km^{-2}·$year^{-1}$ (Fig. 11 d). This falls within the CO_2 flux range observed for active and quiescent worldwide volcanic systems. Further studies are needed to refine these first-order estimates of the mantle-derived CO_2 flux.
8) In addition to asthenospheric ascent, the active seismicity and high heat fluxes (up to 130 mW m^{-2}) characterizing the whole area support the conclusion of a direct volatiles/heat derivation from the mantle and/or from magmatic intrusions scattered throughout the area and linked to mantle upwelling. This elevated transfer of mantle-derived volatiles is interpreted to occur through lithospheric faults that act as regions of enhanced permeability, promoting the migration of fluids throughout the crust. As already discussed elsewhere (e.g., Caracausi and Sulli, 2019; Chiodini et al., 2004; Lee et al., 2019), our study confirms that a significant outgassing of mantle-derived fluids can occur in tectonically active continental regions, even far from active volcanism.

The outcomes of this work offer broader implications and perspectives that help raise fundamental questions for future research. A common conclusion for the different PB areas and the Serbian Vardar zone is that the characterization of the processes that occur during emplacement of fluids in the crust, and their migration through crustal layers, is the key to identifying fluid sources and to obtaining more accurate volatile budgets. Carbon isotope compositions, when combined with noble gas results, constitute a very powerful tool for understanding these processes. The study of carbon isotopic composition, with a focus on ^{14}C, can improve our knowledge of carbon sources and carbon cycles in different settings, potentially allowing for better estimations of the global carbon budget. Furthermore, beyond CO_2 which is the primary focus of this work, it is clear that other major volatile species, such as N_2 and CH_4, are present in some of the studied area. Future studies should characterize the nitrogen and methane isotopes in order to improve our knowledge on the source/s of these species and on the processes occurring within the crust. Based on the identified H_2-rich manifestation, further research on H_2 genesis and potential exploitation in this area should also be conducted. In conclusion, the obtained results contribute to filling a knowledge gap regarding the nature of fluids circulating in this sector of Europe and contribute to a more comprehensive reconstruction of the complex geodynamic evolution and structure of the area.

Declaration of competing interest

The authors declare that they have no known competing financial interests or personal relationships that could have appeared to influence the work reported in this paper.

Appendix A. Supplementary data

Supplementary data to this article can be found online at https://doi.org/10.1016/j.earscirev.2025.105168.

Data availability

Data will be made available on request.

References

Aiuppa, A., Casetta, F., Coltorti, M., et al., 2021. Carbon concentration increases with depth of melting in Earth's upper mantle. Nat. Geosci. 14, 697–703. https://doi.org/10.1038/s41561-021-00797-y.

Alonso, M., Pérez, N.M., Hernández, P.A., Padrón, E., Melián, G., Rodríguez, F., Padilla, G., Barrancos, J., Asensio-Ramos, M., Fridriksson, T., Sumino, H., 2022. Thermal energy and diffuse 4He and 3He degassing released in volcanic-geothermal systems. Renew. Energy 182, 17–31. ISSN 0960-1481. https://doi.org/10.1016/j.renene.2021.10.016.

Bada, G., Horváth, F., Dövényi, P., Szafián, P., Windhoffer, G., Cloetingh, S., 2007. Present-day stress field and tectonic inversion in the Pannonian basin. Glob. Planet. Chang. 58, 165–180.

Baek, G., Kim, J., Lee, C., 2019. A review of the effects of iron compounds on methanogenesis in anaerobic environments. Renew. Sust. Energ. Rev. 113, 109282. ISSN 1364-0321. https://doi.org/10.1016/j.rser.2019.109282.

Balázs, A., Matenco, L., Magyar, I., Horváth, F., Cloetingh, S., 2016. The link between tectonics and sedimentation in back-arc basins: New genetic constraints from the analysis of the Pannonian Basin. Tectonics 35, 1526–1559. https://doi.org/10.1002/2015TC004109.

Ballentine, C.J., Burnard, P., 2002. Production, release and transport of noble gases in the continental crust. Rev. Mineral. Geochem. 47 (1), 481–538. https://doi.org/10.2138/rmg.2002.47.12.

Ballentine, C.J., O'Nions, R.K., Oxburgh, E.R., Horvath, F., Deak, J., 1991. Rare gas constraints on hydrocarbon accumulation, crustal degassing, and groundwater flow in the Pannonian Basin. Earth Planet. Sci. Lett. 105, 229–246.

Ballentine, C.J., O'Nions, R.K., Coleman, M.L., 1996. A magnus opus: helium, neon and argon isotopes in a North Sea oilfield. Geochim. Cosmochim. Acta 60, 831–849.

Ballentine, C.J., Schoell, M., Coleman, D., Cain, B.A., 2001. 300-Myr-old magmatic CO2 in natural gas reservoir of the west Texas Permian basin. Nature 409 (6818), 327–331. https://doi.org/10.1038/35053046.

Barry, P.H., Nakagawa, M., Giovannelli, D., de Moor, J.M., Schrenk, M., Seltzer, A.M., Manini, E., Fattorini, D., di Carlo, M., Regoli, F., Fullerton, K., 2019. Helium, inorganic and organic carbon isotopes of fluids and gases across the Costa Rica convergent margin. Sci. Data 6 (1), 1–8.

Barry, P.H., Negrete-Aranda, R., Spelz, R.M., Seltzer, A.M., Bekaert, D.V., Virrueta, C., Kulongoski, J.T., 2020. Volatile sources, sinks and pathways: a helium-carbon isotope study of Baja California fluids and gases. Chem. Geol. 550 (2020), 119722. https://doi.org/10.1016/j.chemgeo.2020.119722.

Barry, P.H., Bekaer, D.V., Krantz, J.A., Halldórsson, S.A., de Moor, J.M., Fischer, T.P., Werner, C., Kelly, P.J., Seltzer, A.M., Franz, B.P., Kulongoski, J.T., 2021. Helium-carbon systematics of groundwaters in the Lassen Peak Region. Chem. Geol. 584, 120535. ISSN 0009-2541. https://doi.org/10.1016/j.chemgeo.2021.120535.

Belinić, T., Kolínský, P., Stipčević, J., 2021. Shear-wave velocity structure beneath the Dinarides from the inversion of Rayleigh-wave dispersion. Earth Planet. Sci. Lett. 555, 116686. https://doi.org/10.1016/j.epsl.2020.116686.

Bielik, M., Makarenko, I., Starostenko, V., Legostaeva, O., Dererova, J., Šefara, J., Pašteka, R., 2005. New 3D gravity modelling in the Carpathian–Pannonian basin region. Contrib. Geophys. Geodesy. 35, 65–78.
Bielik, M., Kloska, K., Meurers, B., Švancara, J., Wybraniec, S., Fancsik, T., et al., 2006. Gravity anomaly map of the CELEBRATION 2000 region. Geol. Carpath. 57, 145–156.
Bielik, M., Zeyen, H., Starostenko, V., Makarenko, I., Legostaeva, O., Savchenko, S., Dérerová, J., Grinč, M., Godová, D., Pánisová, J., 2022. A review of geophysical studies of the lithosphere in the Carpathian–Pannonian region. Geol. Carpath. 73 (6), 499–516. https://doi.org/10.31577/GeolCarp.73.6.2.
Borović, S., Marković, T., Larva, O., Brkić, Ž., Mraz, V., 2016. Mineral and thermal Waters in the Croatian part of the Pannonian 395 basin. In: Papić, P. (Ed.), Mineral and Thermal Waters of Southeastern Europe. Springer, 31-45, 174 p.
Bracco Gartner, A.J.J., McKenzie, D., 2020. Estimates of the temperature and melting conditions of the Carpathian-Pannonian upper mantle from volcanism and seismology. Geochem. Geophys. Geosyst. 21, e2020GC009334. https://doi.org/10.1029/2020GC009334.
Bräuer, K., Kämpf, H., Niedermann, S., Strauch, G., Tesar, J., 2008. Natural laboratory NW Bohemia: comprehensive fluid studies between 1992 and 2005 used to trace geodynamic processes. Geochem. Geophys. Geosyst. 9, Q04018. https://doi.org/10.1029/2007GC001921.
Bräuer, K., Geissler, W.H., Kämpf, H., Niedermann, S., Rman, N., 2016. Helium and carbon isotope signatures of gas exhalations in the westernmost part of the Pannonian Basin (SE Austria/NE Slovenia): evidence for active lithospheric mantle degassing. Chem. Geol. 422, 60–70. https://doi.org/10.1016/j.chemgeo.2015.12.016.
Broadley, M.W., Bekaert, D.V., Marty, B., Yamaguchi, A., Barrat, J.A., 2020. Noble gas variations in ureilites and their implications for ureilite parent body formation. Geochim. Cosmochim. Acta 270, 325–337. https://doi.org/10.1016/j.gca.2019.11.032.
Brückl, E., Behm, M., Decker, K., Grad, M., Guterch, A., Keller, G.R., Thybo, H., 2010. Crustal structure and active tectonics in the Eastern Alps. Tectonics 29, TC2011. https://doi.org/10.1029/2009tc002491.
Burnard, P., Zimmermann, L., Sano, Y., 2013. The noble gases as geochemical tracers: History and background. In: Burnard, P. (Ed.), The Noble Gases as Geochemical Tracers. Advances in Isotope Geochemistry. Springer, pp. 1–15. https://doi.org/10.1007/978-3-642-28836-4_1.
Buttitta, D., Caracausi, A., Chiaraluce, L., Favara, R., Gasparo Morticelli, M., Sulli, A., 2020. Continental degassing of helium in an active tectonic setting (northern Italy): the role of seismicity. Nat. Sci. Rep. 10, 162. https://doi.org/10.1038/s41598-019-55678-7.
Buttitta, D., Capasso, G., Paternoster, M., Barberio, M.D., Gori, F., Petitta, M., Picozzi, M., Caracausi, A., 2023. Regulation of deep carbon degassing by gas-rock-water interactions in a seismic region of Southern Italy. Sci. Total Environ. 897, 165367. ISSN 0048-9697. https://doi.org/10.1016/j.scitotenv.2023.165367.
Caracausi, A., Paternoster, M., 2015. Radiogenic helium degassing and rock fracturing: a case study of the southern Apennines active tectonic region. J. Geophys. Res. Solid Earth 120, 2200–2211. https://doi.org/10.1002/2014JB011462.
Caracausi, A., Sulli, A., 2019. Outgassing of mantle volatiles in compressional tectonic regime away from volcanism: the role of continental delamination. Geochem. Geophys. Geosyst. 20, 2007–2020. https://doi.org/10.1029/2018GC008046.
Caracausi, A., Favara, R., Italiano, F., Nuccio, P.M., Paonita, A., Rizzo, A., 2005. Active geodynamics of the central Mediterranean Sea: Tensional tectonic evidences in western Sicily from mantle-derived helium. Geophys. Res. Lett. 32, L04312. https://doi.org/10.1029/2004GL021608.
Caracausi, A., Buttitta, D., Picozzi, M., et al., 2022. Earthquakes control the impulsive nature of crustal helium degassing to the atmosphere. Commun. Earth Environ. 3, 224. https://doi.org/10.1038/s43247-022-00549-9.
Chiodini, G., Cardellini, C., Amato, A., Boschi, E., Caliro, S., Frondini, F., Ventura, G., 2004. Carbon dioxide earth degassing and seismogenesis in central and southern Italy. Geophys. Res. Lett. 31.
Chiodini, G., Frondini, F., Cardellini, C., Parello, F., Peruzzi, L., 2000. Rate of diffuse carbon dioxide Earth degassing estimated from carbon balance of regional aquifers: The case of central Apennine. Italy, J. Geophys. Res. 105 (4), 8423–8434. https://doi.org/10.1029/1999JB900355.
Chiodini, G., Valenza, M., Cardellini, C., Frigeri, A., 2008. A new web-based catalogue of Earth degassing sites in Italy. Eos 89 (37), 341342.
Chiodini, G., Caliro, S., Cardellini, C., Frondini, F., Inguaggiato, S., Matteucci, F., 2011. Geochemical evidence for and characterization of CO_2 rich gas sources in the epicentral area of the Abruzzo 2009 earthquakes. Earth Planet. Sci. Lett. 304 (3–4), 389–398. https://doi.org/10.1016/j.epsl.2011.02.016.
Chiodini, G., Cardellini, C., Di Luccio, F., Selva, J., Frondini, F., Caliro, S., Rosiello, A., Beddini, G., Ventura, G., 2020. Correlation between tectonic CO2 Earth degassing and seismicity is revealed by a 10-year record in the Apennines, Italy. Sci. Adv. 6, eabc2938.
Chiodini, G., Cardellini, C., Bini, G., Frondini, F., Caliro, S., Ricci, L., Lucidi, B., 2021a. The carbon dioxide emission as indicator of the geothermal heat flow: review of local and regional applications with a special focus on Italy. Energies 14, 6590. https://doi.org/10.3390/en14206590.
Chiodini, G., Caliro, S., Avino, R., Bini, G., Giudicepietro, F., De Cesare, W., Ricciolino, P., Aiuppa, A., Cardellini, C., Petrillo, Z., Selva, J., Siniscalchi, A., Tripaldi, S., 2021b. Hydrothermal pressure-temperature control on CO2 emissions and seismicity at Campi Flegrei (Italy). J. Volcanol. Geotherm. Res. 414, 107245. ISSN 0377-0273. https://doi.org/10.1016/j.jvolgeores.2021.107245.
Clark, I.D., Fritz, P., 2013. Environmental Isotopes in Hydrogeology. CRC Press.
Conrad, R., 2005. Quantification of methanogenic pathways using stable carbon isotopic signatures: a review and a proposal. Org. Geochem. 36 (5), 739–752. ISSN 0146-6380. https://doi.org/10.1016/j.orggeochem.2004.09.006.
Cornides, I., 1983. The origin of the deep-seated carbon dioxide in the Carpathian Basin: implications of water-rock interactions. In: 4th International Symposium of Water-Rock Interaction, Misasa (Japan). Extended Abstracts 97-98.
Cornides, I., Kecskés, A., 1982. Deep-seated carbon dioxide in Slovakia: the problem of its origin. Geol. Zbornik-Geol. Carpathica 32, 183–190.
Csontos, L., 1995. Tertiary tectonic evolution of the intra-Carpathian area: a review. Acta Vulcanol. 7, 1–13.
Erdelyi, M., 1976. Outlines of the hydrodynamics and hydrochemistry of the Pannonian Basin. Acta Geol. Acad. Sci. Hung. 20 (3-4), 287–309.
Faccenna, C., Becker, T.W., Auer, L., Billi, A., Boschi, L., Brun, J.P., et al., 2014. Mantle dynamics in the Mediterranean. Rev. Geophys. 52, 283–332. https://doi.org/10.1002/2013RG000444.
Fiket, Ž., Rožmarić, M., Krmpotić, M., Petrinec, B., 2015. Trace and rare Earth element geochemistry of croatian thermal waters. Int. J. Environ. Res. 9 (2), 595–604. https://doi.org/10.22059/ijer.2015.934.
Fodor, L., Csontos, L., Bada, G., Györfi, I., Benkovics, L., 1999. Tertiary tectonic evolution of the Pannonian basin system and neighbouring orogens: a new synthesis of paleostress data. In: Durand, B., et al. (Eds.), The Mediteranean Basins: Tertiary Extension Within the Alpine Orogen, pp. 295–334. Geol. Soc., London.
Foley, S.F., Fischer, T.P., 2017. An essential role for continental rifts and lithosphere in the deep carbon cycle. Nat. Geosci. 10, 897–902. https://doi.org/10.1038/s41561-017-0002-7.
Frondini, F., Cardellini, C., Caliro, S., Beddini, G., Rosiello, A., Chiodini, G., 2018. Measuring and interpreting CO_2 fluxes at regional scale: the case of the Apennines, Italy. J. Geol. Soc. 176 (2), 408–416. https://doi.org/10.1144/jgs2017-169.
Frunzeti, N., 2013. Geogenic Emissions of Greenhouse Gases in the Southern Part of the Eastern Carpathians (Doctoral Dissertation). Babes-Bolyai University, Faculty of Environmental Science and Engineering (in Romanian).
Gautheron, C., Moreira, M., 2002. Helium signature of the subcontinental lithospheric mantle. Earth Planet. Sci. Lett. 199 (1–2), 39–47. https://doi.org/10.1016/S0012-821X(02)00563-0.
Gautheron, C., Moreira, M., Allègre, C., 2005. He, Ne and Ar composition of the European lithospheric mantle. Chem. Geol. 217 (1–2), 97–112. ISSN 0009-2541,. https://doi.org/10.1016/j.chemgeo.2004.12.009.
Gilfillan, S.M.V., Lollar, B.S., Holland, G., Blagburn, D., Stevens, S., Schoell, M., et al., 2009. Solubility trapping in formation water as dominant CO2 sink in natural gas fields. Nature 458 (7238), 614–618. https://doi.org/10.1038/nature07852.
Godova, D., Bielik, M., Hrubcova, P., Šimonova, B., Dererova, J., Pašteka, R., 2021. Lithospheric density model along the CEL09 profile and its geological implications. Geol. Carpath. 72 (6), 447–460. https://doi.org/10.31577/GeolCarp.72.6.1.
Grenerczy, Gy., Sella, G.F., Stein, S., Kenyeres, A., 2005. Tectonic implications of the GPS velocity field in the northern Adriatic region. Geophys. Res. Lett. 32, L16311.
Güleç, N., Hilton, D.R., 2006. Helium and heat distribution in western Anatolia, Turkey: relationship to active extension and volcanism. In: Postcollisional Tectonics and Magmatism in the Mediterranean Region and Asia, Yildirim Dilek, Spyros Pavlides. https://doi.org/10.1130/2006.2409(16).
Guterch, A., Grad, M., Špičák, A., Brückl, E., Hegedüs, E., Keller, G.R., Thybo, H., CELEBRATION, 2000a. ALP 2002 and SUDETES 2003 working groups 2003a: special contributions: an overview of recent seismic refraction experiments in central Europe. Stud. Geophys. Geod. 47, 651–657. https://doi.org/10.1023/A:1024775921231.
Guterch, A., Grad, M., Špičák, A., Brückl, E., Hegedüs, E., Keller, G.R., Thybo, H., CELEBRATION, 2000b. ALP 2002 and SUDETES 2003 working groups 2003b: special contributions: an overview of recent seismic refraction experiments in central Europe. Stud. Geophys. Geod. 47, 659–669. https://doi.org/10.1023/A:1024728005301.
Heuer, V.B., Inagaki, F., Morono, Y., Kubo, Y., Spivack, A.J., Viehweger, B., Treude, T., Beulig, F., Schubotz, F., Tonai, S., Bowden, S.A., Cramm, M., Henkel, S., Hirose, T., Homola, K., Hoshino, T., Ijiri, A., Imachi, H., Kamiya, N., Kaneko, M., Lagostina, L., Manners, H., McClelland, H.-L., Metcalfe, K., Okutsu, N., Pan, D., Raudsepp, M.J., Sauvage, J., Tsang, M.-Y., Wang, D.T., Whitaker, E., Yamamoto, Y., Yang, K., Maeda, L., Adhikari, R.R., Glombitza, C., Hamada, Y., Kallmeyer, J., Wendt, J., Wormer, L., Yamada, Y., Kinoshita, M., Hinrichs, K.-U., 2020. Temperature Limits to Deep Subseafloor Life in the Nankai Trough Subduction Zone. Science 370 (6521), 1230–1234.
Hiett, C.D., Newell, D.L., Jessup, M.J., 2021. 3He evidence for fluid transfer and continental hydration above a flat slab. Earth Planet. Sci. Lett. 556, 116722. ISSN 0012-821X. https://doi.org/10.1016/j.epsl.2020.116722.
Holland, G., Gilfillan, S., 2013. Application of noble gases to the viability of CO2 storage. In: Burnard, P. (Ed.), The Noble Gases as Geochemical Tracers. Advances in Isotope Geochemistry. Springer, Berlin, Heidelberg. https://doi.org/10.1007/978-3-642-28836-4_8.
Horváth, F., Musitz, B., Balázs, A., Végh, A., Uhrin, A., Nádor, A., et al., 2015. Evolution of the Pannonian basin and its geothermal resources. Geothermics 53, 328–352. https://doi.org/10.1016/j.geothermics.2014.07.009.
Horváth, F., Dulić, I., Vranković, A., Koroknai, B., Tóth, T., Wórum, G., Kovács, G., 2018. Overview of geologic evolution and hydrocarbon generation of the Pannonian Basin. Interpretation 6, SB111–SB122. https://doi.org/10.1190/int-2017-0100.1.
Huismans, R.S., Podladchikov, Y.Y., Cloetingh, S., 2001. Dynamic modelling of the transition from passive to active rifting, application to the Pannonian basin. Tectonics 20 (6), 1021–1039.
Hurter, S., Haenel, R., 2002. Atlas of Geothermal Resources in Europe. Office for Official Publications of the European Communities, Luxembourg.

Ionescu, A., Baciu, C., Kis, B.-M., Sauer, P.E., 2017. Evaluation of dissolved light hydrocarbons in different geological settings in Romania. Chem. Geol. 469, 230–245. https://doi.org/10.1016/j.chemgeo.2017.04.017.

Italiano, F., Kis, B.M., Baciu, C., Ionescu, A., Harangi, S., Palcsu, L., 2017. Geochemistry of dissolved gases from the eastern Carpathians- Transylvanian Basin boundary. Chem. Geol. 469, 117–128. https://doi.org/10.1016/j.chemgeo.2016.12.019.

Kalmár, D., Petrescu, L., Stipčević, J., Balázs, A., János Kovács, I., the AlpArray and PACASE Working Groups, 2023. Lithospheric structure of the circum-Pannonian region imaged by S-to-P receiver functions. Geochem. Geophys. Geosyst. 24, e2023GC010937. https://doi.org/10.1029/2023GC010937.

Kimani, C.N., Kasanzu, C.H., Tyne, R.L., Mtili, K.M., Byrne, D.J., Kazimoto, E.O., Hillegonds, D.J., Ballentine, C.J., Barry, P.H., 2021. He, Ne, Ar and CO2 systematics of the Rungwe Volcanic Province, Tanzania: Implications for fluid source and dynamics. Chem. Geol. 586, 120584. ISSN 0009-2541. https://doi.org/10.1016/j.chemgeo.2021.120584.

Konecny, V., Kovac, M., Lexa, J., Sefara, J., 2002. Neogene evolution of the Carpatho-Pannonian region: an interplay o fsubduction and back-arc uprise in the mantle. EGU St. Mueller Spec. Publ. Ser. 1, 105–123.

Koptev, A., Cloetingh, S., Kovács, I.J., Gerya, T., Ehlers, T.A., 2021. Controls by rheological structure of the lithosphere on the temporal evolution of continental magmatism: inferences from the Pannonian Basin system. Earth Planet. Sci. Lett. 565, 116925. ISSN 0012-821X. https://doi.org/10.1016/j.epsl.2021.116925.

Koroknai, B., Wórum, G., Tóth, T., Koroknai, Z., Fekete-Németh, V., Kovács, G., 2020. Geological deformations in the Pannonian Basin during the neotectonic phase: new insights from the latest regional mapping in Hungary. Earth Sci. Rev. 211, 103411. ISSN 0012-8252. https://doi.org/10.1016/j.earscirev.2020.103411.

Kulongosky, J.T., Hilton, D.R., Izbicki, J.A., 2005. Source and movement of helium in the eastern Morongo groundwater basin: the influence of regional tectonics on crustal and mantle helium fluxes. Geochim. Cosmochim. Acta 69, 3857–3872. https://doi.org/10.1016/j.gca.2005.03.001.

Kulongosky, J.T., Hilton, D.R., Barry, P.H., Bradley, K.E., Darren, H., Kenneth, B., 2013. Volatilefluxes through the Big Bend sectionof the San Andreas Fault, California: Helium and carbon-dioxide systematics. Chem. Geol. 339, 92–102. https://doi.org/10.1016/j.chemgeo.2012.09.007.

Labidi, J., Barry, P.H., Bekaert, D.V., Broadley, M.W., Marty, B., Giunta, T., et al., 2020. Hydrothermal 15N15N abundances constrain the origins of mantle nitrogen. Nature 580, 367–371. https://doi.org/10.1038/s41586-020-2173-4.

Lee, C.-T., Jiang, H., Dasgupta, R., Torres, M., 2019. A framework for understanding whole-Earth carbon cycling. In: Orcutt, B.N., Daniel, I., Dasgupta, R. (Eds.), Deep Carbon: Past to Present. Cambridge University Press, Cambridge, pp. 313–357.

Lenkey, L., Dövényi, P., Horváth, F., Cloetingh, S.A.P.L., 2002. Geothermics of the Pan-Nonian Basin and its Bearing on the Neotectonics, 3. EGU Stephan Mueller Special Publication Series, pp. 1–12. https://doi.org/10.5194/smsps-3-29-2002.

Mamyrin, B.A., Tolstikhin, I.N., 1984. Helium Isotopes in Nature. Developments in Geochemistry. Elsevier Science Ltd.

Markušić, S., 2008. Seismicity of croatia. In: Husebye, E.S. (Ed.), Earthquake Monitoring and Seismic Hazard Mitigation in Balkan Countries, NATO Science Series: IV: Earth and Environmental Sciences, 81. Springer, Dordrecht. https://doi.org/10.1007/978-1-4020-6815-7_5.

Markušić, S., Stanko, D., Penava, D., Ivančić, I., Bjelotomić Oršulić, O., Korbar, T., Sarhosis, V., 2021. Destructive M6.2 Petrinja Earthquake (Croatia) in 2020—preliminary Multidisciplinary Research. Remote Sens. 13 (6), 1095. https://doi.org/10.3390/rs13061095.

Marty, B., Almayrac, M., Barry, P.H., Bekaert, D.V., Broadley, M.W., Byrne, D.J., et al., 2020. An evaluation of the C/N ratio of the mantle from natural CO2-rich gas analysis: Geochemical and cosmochemical implications. Earth Planet. Sci. Lett. 551 (2020), 116574. https://doi.org/10.1016/j.epsl.2020.116574.

Matenco, L., Radivojevic, D., 2012. On the formation and evolution of the Pannonian Basin: constraints derived from the structure of the junction area between the Carpathians and Dinarides. Tectonics 31. https://doi.org/10.1029/2012TC003206.

McIntosh, J.C., Warwick, P.D., Martini, A.M., Osborn, S.G., 2010. Coupled Hydrology and Biogeochemistry of Paleocene–Eocene Coal Beds, Northern Gulf of Mexico. Geol. Soc. Am. Bull. 122 (7–8), 1248–1264.

Merten, S., Matenco, L., Foeken, J.P.T., Stuart, F.M., Andriessen, P.A.M., 2010. From nappe stacking to out-of-sequence postcollisional deformations: cretaceous to Quaternary exhumation history of the SE Carpathians assessed by low-temperature thermochronology. Tectonics 29, TC3013. https://doi.org/10.1029/2009TC002550.

Milkov, A.V., 2020. In: Wilkes, H. (Ed.), In Hydrocarbons, Oils and Lipids: Diversity, Origin, Chemistry and Fate. Springer, pp. 613–622.

Mutlu, H., Güleç, N., Hilton, D.R., 2008. Helium–carbon relationships in geothermal fluids of western Anatolia, Turkey. Chem. Geol. 247 (1–2), 305–321. ISSN 0009-2541. https://doi.org/10.1016/j.chemgeo.2007.10.021.

Nádor, A., Sebess-Zilahi, L., Rotár-Szalkai, Á., Gulyás, Á., Markovic, T., 2019. New methods of geothermal potential assessment in the Pannonian basin. Neth. J. Geosci. 98, e10. https://doi.org/10.1017/njg.2019.7.

Newell, D.L., Jessup, M.J., Cottle, J.M., Hilton, D.R., Sharp, Z.D., Fischer, T.P., 2008. Aqueous and isotope geochemistry of mineral springs along the southern margin of the Tibetan plateau: implications for fluid sources and regional degassing of CO2. Geochem. Geophys. Geosyst. 9, Q08014. https://doi.org/10.1029/2008GC002021.

O'Nions, R.K., Oxburgh, E.R., 1988. Helium, volatile fluxes and the development of continental crust. Earth Planet. Sci. Lett. 90 (3), 331–334. https://doi.org/10.1016/0012-821X(88)90134-3.

Ottlik, P., Galfi, J., Horvath, F., 1981. The low enthalpy geothermal resource of the Pannonian Basin, Hungary. In: Rybach, L., Muffler, L.J.P. (Eds.), Geothermal Systems. Wiley, New York, N.Y, pp. 221–245.

Ozima, M., Podosek, F.A., 2002. Noble Gas Geochemistry. Cambridge University Press, p. 286.

Palcsu, L., Vetö, I., Futó, I., Vodila, G., Papp, L., Major, Z., 2014. In-reservoir mixing of mantle-derived CO2 and metasedimentary CH4–N2 fluids — noble gas and stable isotope study of two multistacked fields (Pannonian Basin System, W-Hungary). Mar. Pet. Geol. 54, 216–227.

Poreda, R.J., Jenden, P.D., Kaplan, I.R., Craig, H., 1986. Mantle helium in Sacramento basin natural gas wells. Geochim. Cosmochim. Acta 50 (12), 2847–2853. ISSN 0016-7037,. https://doi.org/10.1016/0016-7037(86)90231-0.

Randazzo, P., Caracausi, A., Aiuppa, A., Cardellini, C., Chiodini, G., D'Alessandro, W., Li Vigni, L., Papic, P., Marinkovic, G., Ionescu, A., 2021. Active degassing of deeply sourced fluids in Central Europe: new evidences from a geochemical study in Serbia. Geochem. Geophys. Geosyst. 22 (11). https://doi.org/10.1029/2021gc010017.

Randazzo, P., Caracausi, A., Aiuppa, A., Cardellini, C., Chiodini, G., Apollaro, C., Paternoster, M., Rosiello, A., Vespasiano, G., 2022. Active degassing of crustal CO2 in areas of tectonic collision: a case study from the Pollino and Calabria sectors (Southern Italy). Front. Earth Sci. China 10, 873. https://doi.org/10.3389/feart.2022.946707.

Reeve, J.N., Nolling, J., Morgan, R.M., Smith, D.R., 1997. Methanogenesis: genes, genomes, and who's on first? J. Bacteriol. 179 (19), 5975–5986.

Ren, Y., others, 2013. Crustal structure of the Carpathian–Pannonian region from ambient noise tomography. Geophys. J. Int. 195 (2), 1351–1369. https://doi.org/10.1093/gji/ggt316.

Rizzo, A.L., Pelorosso, B., Coltorti, M., Ntaflos, T., Bonadiman, C., Matusiak-Małek, M., et al., 2018. Geochemistry of noble gases and CO2 in fluid inclusions from lithospheric mantle beneath Wilcza Góra (lower Silesia, Southwest Poland). Front. Earth Sci. 6, 215. https://doi.org/10.3389/feart.2018.00215.

Rman, N., Bălan, L.L., Bobovečki, I., et al., 2020. Geothermal sources and utilization practice in six countries along the southern part of the Pannonian basin. Environ. Earth Sci. 79, 1. https://doi.org/10.1007/s12665-019-8746-6.

Rufino, F., Cuoco, E., Busico, G., et al., 2021. Deep carbon degassing in the Matese massif chain (Southern Italy) inferred by geochemical and isotopic data. Environ. Sci. Pollut. Res. 28, 46614–46626. https://doi.org/10.1007/s11356-020-11107-1.

Sano, Y., Marty, B., 1995. Origin of carbon in fumarolic gas from island arcs. Chem. Geol. 119, 265–274. https://doi.org/10.1016/0009-2541(94)00097-R.

Sano, Y., Tominaga, T., Williams, S.N., 1997. Secular variations of helium and carbon isotopes at Galeras volcano, Colombia. J. Volcanol. Geotherm. Res. 77 (1–4), 255–265. https://doi.org/10.1016/S0377-0273(96)00098-4.

Sarbu, S., Aerts, J.W., Flot, J.F., Van Spanning, R.J.M., Baciu, C., Ionescu, A., et al., 2018. Sulfur Cave (Romania), an extreme environment with microbial mats in a CO2-H2S/O gas chemocline dominated by mycobacteria. Int. J. Speleol. 47 (2), 173–187. https://doi.org/10.5038/1827-806x.47.2.2164.

Schmid, S.M., Fügenschuh, B., Kounov, A., Matenco, L., Nievergelt, P., Oberhänsli, R., et al., 2020. Tectonic units of the Alpine collision zone between Eastern Alps and Western Turkey. Gondwana Res. 78, 308–374. https://doi.org/10.1016/j.gr.2019.07.005.

Sherwood, Lollar B., O'Nions, R.K., Ballentine, C.J., 1994. Helium and neon isotope systematics in carbon dioxide-rich and hydrocarbon-rich gas reservoirs. Geochim. Cosmochim. Acta 58, 5279–5290.

Sherwood, Lollar B., Ballentine, C.J., O'Nions, R.K., 1997. The fate of mantle-derived carbon in a continental sedimentary basin: Integration of C/he relationships and stable isotope signatures. Geochim. Cosmochim. Acta 61, 2295–2307. https://doi.org/10.1016/S0016-7037(97)00083-5.

Szafian, P., Horvath, F., Cloetingh, S.A.P.L., 1997. Gravity contraints on the crustal structure and slab evolution along a Transcarpathian transect. Tectonophysics 272, 233–248.

Takai, K., Nakamura, K., Toki, T., Tsunogai, U., Miyazaki, M., Miyazaki, J., Hirayama, H., Nakagawa, S., Nunoura, T., Horikoshi, K., 2008. Cell Proliferation at 122°C and Isotopically Heavy CH4 production by a Hyperthermophilic Methanogen under High-pressure Cultivation. Proc. Natl. Acad. Sci. USA 105 (31), 10949–10954.

Tamburello, G., Pondrelli, S., Chiodini, G., Rouwet, D., 2018. Global-scale control of extensional tectonics on CO2 earth degassing. Nat. Commun. 9, 4608. https://doi.org/10.1038/s41467-018-07087-z.

Tari, G., Dövényi, P., Dunkl, I., Horváth, F., Lenkey, L., Stefanescu, M., Szafián, P., Tóth, T., 1999. Lithospheric structure of the Pannonian basin derived from seismic, gravity and geothermal data. Geol. Soc. Lond. Spec. Publ. 156, 215–250. https://doi.org/10.1144/GSL.SP.1999.156.01.12.

Tašarova, A., Afonso, J.C., Bielik, M., Gotze, H.J., Hok, J., 2009. The lithospheric structure of the Western Carpathian–Pannonian Basin region based on the CELEBRATION 2000 seismic experiment and gravity modelling. Tectonophysics 475 (3–4), 454–469. https://doi.org/10.1016/j.tecto.2009.06.003.

Torgersen, T., 1993. Defining the role of magmatism in extensional tectonics: Helium 3 fluxes in extensional basins. J. Geophys. Res. 98 (B9), 16257–16269. https://doi.org/10.1029/93JB00891.

Torgersen, T., 2010. Continental degassing flux of 4He and its variability. Geochem. Geophys. Geosyst. 11, Q06002. https://doi.org/10.1029/2009GC002930.

Tóth, J., Almási, I., 2001. Interpretation of observed fluid potential patterns in a deep sedimentary basin under tectonic compression: Hungarian Great Plain, Pannonian Basin. Geofluids 1, 11–36. https://doi.org/10.1046/j.1468-8123.2001.11004.x.

Tóth, L., Györi, E., Mónus, P., Zsíros, T., 2006. Seismic Hazard in the Pannonian Region. In: Pinter, N., Grenerczy, G., Weber, J., Stein, S., Medak, D. (Eds.), The Adria Microplate: GPS Geodesy, Tectonics, and Hazards, NATO ARW Series, 61. Springer Verlag, pp. 369–384.

Tóth, L., Mónus, P., Bus, Z., Györi, E., 2008. Seismicity of the Pannonian Basin (2008). In: Husebye, E.S. (Ed.), Earthquake Monitoring and Seismic Hazard Mitigation in Balkan Countries. Springer Science + Business Media B.V.

Tyne, R.L., Barry, P.H., Lawson, M., et al., 2021. Rapid microbial methanogenesis during CO2 storage in hydrocarbon reservoirs. Nature 600, 670–674. https://doi.org/10.1038/s41586-021-04153-3.

Tyne, R.L., Barry, P.H., Lawson, M., Lloyd, K.G., Giovannelli, D., Summers, Z.M., Ballentine, C.J., 2023. Identifying and understanding microbial methanogenesis in CO2 storage. Environ. Sci. Technol. 57 (26), 9459–9473. https://doi.org/10.1021/acs.est.2c08652.

Vető, I., Futó, I., Horváth, I., Szántó, Z., 2004. Late and deep fermentative methanogenesis as reflected in the H-C-O-S isotopy of the methane-water system in deep aquifers of the Pannonian Basin (SE Hungary). Org. Geochem. 35 (6), 713–723. ISSN 0146-6380,. https://doi.org/10.1016/j.orggeochem.2004.02.004.

Vető, I., Csizmeg, J., Sajgó, C., 2014. Mantle-related CO2, metasedimentary HC-N2 gas and oil traces in the Répcelak and Mihályi accumulations, W-Hungary — mixing of three fluids of very different origin. Central Eur. Geol. 57 (1), 53–69. https://doi.org/10.1556/ceugeol.57.2014.1.3.

Vinson, David, S., Blair, Neal, E., Ritter, Daniel, J., Martini, Anna, M., McIntosh, Jennifer, C., 2019. Carbon mass balance, isotopic tracers of biogenic methane, and the role of acetate in coal beds: Powder River Basin (USA). Chem. Geol. 530, 119329. https://doi.org/10.1016/j.chemgeo.2019.119329. ISSN 0009-2541.

Werner, C., Fischer, T., Aiuppa, A., Edmonds, M., Cardellini, C., Carn, S., Allard, P., 2019. Carbon dioxide emissions from Subaerial Volcanic Regions: Two decades in review. In: Orcutt, B., Daniel, I., Dasgupta, R. (Eds.), Deep Carbon: Past to Present. Cambridge University Press, Cambridge, pp. 188–236.

Whiticar, Michael J., 1999. Carbon and hydrogen isotope systematics of bacterial formation and oxidation of methane. Chem. Geol. 161 (1–3), 291–314. https://doi.org/10.1016/S0009-2541(99)00092-3. ISSN 0009-2541.

Zhang, J., Quay, P.D., Wilbur, D.O., 1995. Carbon isotope fractionation during gas-water exchange and dissolution of CO2. Geochim. Cosmochim. Acta 59, 107–114.

Zhang, M., Xu, S., Zhou, X., Caracausi, A., Sano, Y., Guo, Z., Zheng, G., Lang, Y., Liu, C., 2021. Deciphering a mantle degassing transect related with India-Asia continental convergence from the perspective of volatile origin and outgassing. Geochim. Cosmochim. Acta 310, 61–78. ISSN 0016-7037,. https://doi.org/10.1016/j.gca.2021.07.010.

Zhou, Z., Ballentine, C.J., Kipfer, R., Schoell, M., Thibodeaux, S., 2005. Noble gas tracing of groundwater/coalbed methane interaction in the San Juan Basin, USA. Geochim. Cosmochim. Acta 69 (23), 5413–5428.

Živković, S., Kolbah, S., Škrlec, M., 2016. Croatia country update. In: European Geothermal Congress 2016, Strasbourg, France, 19–24 Sept 2016.

Zsíros, T., 2003a. Earthquake activity and hazard in the Carpathian basin I. Acta Geod. Geoph. Hung. 38 (3), 345–362.

Zsíros, T., 2003b. Earthquake activity and hazard in the Carpathian basin II. Acta Geod. Geoph. Hung. 38 (4), 445–465.